

MASTER

ANNUAL REPORT

on

CONTRACT AEC AT(11-1)34 P107B

AT03-76 ER 10107

between

THE U.S. ATOMIC ENERGY COMMISSION

and

THE UNIVERSITY OF CALIFORNIA, RIVERSIDE

Prepared by: W. H. Barkas

May 1967

Legal Notice

This report was prepared as an account of Government sponsored work. Neither the United States, nor the Commission, nor any person acting on behalf of the Commission:

A. Makes any warranty or representation, expressed or implied, with respect to the accuracy, completeness, or usefulness of the information contained in this report, or that the use of any information, apparatus, method, or process disclosed in this report may not infringe privately owned rights; or

B. Assumes that any liabilities with respect to the use of, or for damages resulting from the use of any information, apparatus, method or process disclosed in this report.

As used in the above, "person acting on behalf of the Commission" includes any employee or contractor of the Commission, or employee of such contractor, to the extent that such employee or contractor of the Commission, or employee of such contractor prepares, disseminates, or provides access to, any information pursuant to his employment or contract with the Commission, or his employment with such contractor.

DISCLAIMER
This book was prepared as an account of work sponsored by an agency of the United States Government. Neither the United States Government nor any agency thereof, nor any of their employees, makes any warranty, express or implied, or assumes any legal liability or responsibility for the accuracy, completeness, or usefulness of any information, apparatus, product, or process disclosed, or represents that its use would not infringe privately owned rights. Reference herein to any specific commercial product, process, or service by trade name, trademark, manufacturer, or otherwise, does not necessarily constitute or imply its endorsement, recommendation, or favoring by the United States Government or any agency thereof. The views and opinions of authors expressed herein do not necessarily state or reflect those of the United States Government or any agency thereof.

DISTRIBUTION OF THIS DOCUMENT IS UNLIMITED

[Handwritten mark]

34-107-46

DISCLAIMER

This report was prepared as an account of work sponsored by an agency of the United States Government. Neither the United States Government nor any agency Thereof, nor any of their employees, makes any warranty, express or implied, or assumes any legal liability or responsibility for the accuracy, completeness, or usefulness of any information, apparatus, product, or process disclosed, or represents that its use would not infringe privately owned rights. Reference herein to any specific commercial product, process, or service by trade name, trademark, manufacturer, or otherwise does not necessarily constitute or imply its endorsement, recommendation, or favoring by the United States Government or any agency thereof. The views and opinions of authors expressed herein do not necessarily state or reflect those of the United States Government or any agency thereof.

DISCLAIMER

Portions of this document may be illegible in electronic image products. Images are produced from the best available original document.

Summary

Work that has been carried out in several areas of High Energy Physics is described. Visual techniques are used. For the study of the three-pion decay of the K^+ meson, bubble chamber and emulsion methods are used to complement each other, particularly for the τ' mode. Several separate bubble chamber experiments in π^+p , $\bar{p}p$ and K^-p interactions are also described, and the large effort devoted to computer reprogramming for the data analysis indicated. Two emulsion research projects are also described which have for their purpose the study of electromagnetic processes induced by 16 BeV electrons and the study of hypernuclei by K^- mesons. For the latter work high speed computer methods have been successfully applied to the analysis of the product hypernuclei. These programs of work have not been under way long enough for the main results yet to be available, but some preliminary data have been published and several reports on data analysis and related subjects have been prepared.

The work is carried out by a staff of seven Ph.D. physicists, seven graduate students, and a variable number of undergraduate scanners.

ANNUAL PROGRESS REPORT

Introduction

At the time this is written the work of this contract has been under way nearly two years. A year ago we could report that substantial progress had been made on Program A described below. Now we can report much more work on that program, and considerable activity on new programs which we have designated B, C, D, E and F.

The work is being led by seven members of the faculty and research associates in the department of physics. Seven graduate students are engaged in the work, and about 24 undergraduate students are employed (usually part-time). We have expanded into additional space as staff and new equipment were acquired.

Computer programs have been revised so that they will run on our IBM 7040 computer. They are as follows:

- Panel: an intermediate program which takes the measurement data of bubble chamber films and performs numerous checks.
- TVGP: a three-view geometrical reconstruction program for converting two-dimensional measurement into spatial variables.
- Squaw: a kinematic program which tries and compares various mass hypotheses for a given event configuration.
- Arrow: a post-kinematic program with which various histograms and theory-fittings can be carried out.
- LSQVMT: a least-square fitting routine which can handle up to 40 parameters and 10 independent variables.

A number of shorter programs have been written for specific calculations.

Program A - Three-Pion Decay Of The K^+ Meson

D. Davison, S. Y. Fung, R. B. Bacastow, D. A. Evans,

L. E. Porter, R. T. Pu and W. H. Barkas

I. Introduction

Some questions which are posed in connection with three-pion decay are the following:

- a) Is the dependence of the amplitude on the odd pion momentum intrinsic or is it a final state effect?
- b) Has the dependence of the weak-interaction K^+ decay amplitude on the odd pion momentum the same origin as the effect in the case of the electromagnetic decay of the η meson? (The effect also is seen in the π^0 momentum of $K_2^0 \rightarrow \pi^+ + \pi^- + \pi^0$ decay.)
- c) Is the $|\Delta I| = \frac{1}{2}$ law broken measurably in these processes?
- d) Is the predicted threshold effect of the τ mode detectable in the upper part of the τ' spectrum?

The research we are carrying out is directed toward improving the experimental data which provide the empirical bases for answering these questions. With more and better data one can make detailed comparisons with the current algebra model, and in conjunction with experiments on the pion-pion interaction, determine what role is played by the final state scatterings. In parallel with this experimental work Dunn and Ramachandran¹ have extended the theoretical understanding of final state processes by considering multiple scatterings.

Our measurements of the τ'/τ branching ratio and the odd pion energy spectra (applying Weinberg's analysis²) provide tests of the $|\Delta I| = \frac{1}{2}$ law. In addition, with the improved statistics and reduced systematic errors of this experiment we are looking for the "cusp phenomenon"³ at the τ threshold.

The τ and τ' decay modes were discovered using emulsion detection, and they have been subjects of study with it for many years. More recently use has been made of bubble chambers so that large statistics could be more easily obtained. However, neither of the instruments has good efficiency or is capable of reliable measurements over the whole spectrum of secondary pions from τ' decay.

The present program originated as two separate phases at the Lawrence Radiation Laboratory, but was transferred and considerably expanded on the Riverside campus of the University of California. We realized that for this task the bubble chamber and emulsion admirably supplement each other, and we use them in conjunction. In the important energy interval of 0 - 20 MeV the emulsion measurements are good, and in the interval above 10 or 15 MeV the bubble chamber yields large statistics and the measurements are reliable. Of course, the scanning efficiency for neither instrument is 100 percent at any energy so that special efficiency studies have been made for each. These will be discussed in section II. The scanning efficiencies for τ events are high for both instruments, but require some analysis which also will be included in section II.

The final state of three pions is one which must be symmetric in the ispin coordinates of the mesons. Thus, with the assumption that in the final state the pions have no relative angular momentum, the total ispin must be 1 or 3, while the two like pions may exist only in ispin states of 0 or 2.

Suppose the amplitude for τ and τ' decay are respectively $A(r, \theta)$, and $B(r, \theta)$. We define r and θ as coordinates on a Dalitz plot such that the kinetic energies T_1 and T_2 of the like pions are

$$T_1 = 1/3Q[1 + r \cos (\frac{2\pi}{3} - \theta)]$$

$$T_2 = 1/3Q[1 + r \cos (\frac{2\pi}{3} + \theta)],$$

while the energy T_3 of the unlike pion is

$$T_3 = 1/3Q[1 + r \cos \theta].$$

The Q -values are respectively 75.04 MeV and 84.25 MeV for the τ and τ' decays.

Because of the symmetry of the two like pions the decay amplitudes must be symmetric in T_1 and T_2 . One may therefore expand the decay amplitudes following Weinberg as Fourier Series in cosines.

$$A = \sum_l a_l(r) \cos l\theta$$

and
$$B = \sum_l b_l(r) \cos l\theta$$

The expansion may first be made quite naturally in powers of $(3T_3 - Q) = Qr \cos \theta$, and subsequently converted to a Fourier Series. Now if the final state is pure ispin 1,

$$A(r, \theta) = -[B(r, \frac{2\pi}{3} + \theta) + B(r, \frac{4\pi}{3} + \theta)]$$

and
$$B(r, \theta) = \frac{1}{2}[A(r, \theta) - A(r, \frac{2\pi}{3} + \theta) - A(r, \frac{4\pi}{3} + \theta)]$$

These requirements impose conditions on the coefficients a_i and b_i ; e.g. $a_0 = -2b_0$, and $a_1 = b_1$, so that in the linear approximation, valid when ϵ is small,

$$|A(r, \theta)|^2 = a_0^2(1 + \epsilon \cos \theta)$$

$$|B(r, \theta)|^2 = a_0^2/4(1 - 2\epsilon \cos \theta)$$

Thus, aside from the density of states factor, the $|\Delta I| = \frac{1}{2}$ rule predicts the τ' decay rate to be $\frac{1}{4}$ that of the τ rate and the variation of the τ' decay probability on T_3 to be twice as rapid and opposite in sign. When examined in greater detail a violation of the first prediction would detect the presence of $\Delta I = 5/2$ transitions, and of the second, $\Delta I = 3/2$. A total ispin of 2 is also barred by symmetry arguments, as noted above.

Second degree and higher power terms in the expansion of the matrix element are possible, and may provide information on the $\pi\pi$ final state interaction. Our data on preliminary analysis indicates the presence of a second degree term.

II. Data Acquisition and Reduction

The employment of both emulsion and bubble chamber as complementary instruments with which to span the full range of odd pion energies was described briefly in section I. The data were in fact gathered fairly independently by the respective

research groups, with sufficient coordination to be able eventually to match the results, even if necessary, using a small energy interval over which the two methods were equally effective. Hence the initial stages of data collection and reduction will be treated individually herein.

A. Bubble Chamber Phase

The K^+ decay experiment which was the source of data for the present study has been described in detail previously.⁴ The Berkeley 30-inch heavy liquid bubble chamber, filled with Freon I (C_3F_8), was used to stop K^+ mesons produced with the Bevatron. Some three million stopping K^+ tracks were photographed in roughly 240,000 exposures. Of the 240 rolls of film about 40% were selected for this study, taking care to exclude any rolls scanned in an earlier τ' project.⁵ So far 71 rolls of the 105 in our sample have been scanned for τ' events, but to date just 37 of these have been scanned for τ events. These two modes of K^+ decay will be discussed separately below.

1. τ' Data

The τ' mode of K decay is recognized by the $\pi^+ \rightarrow \mu^+ \rightarrow e^+$ chain of decays, characterized by a 1.4 mm μ -kink. A τ' event is distinguishable from a $K\pi^2$ event because the maximum range of a π^+ from the former mode, 10.1 cm, is markedly less than the unique range, 31.2 cm, in the latter mode; the rare radiative $K\pi^2$ mode remained a source of background, however. Another source of background which was present was the $K\mu_3$ event with a μ -kink simulated by a μ -scatter at the track's end. If the π^+ track from a τ' decay were less than 5 cm in length, the ionization

density was not clearly different than that of a stopping K^+ , so that it was necessary to exclude all potential events whose (apparent) K^+ track suffered a scatter in the last 5 cm of its path. Thus a scattered K^+ decay via the $K\mu_3$ mode with a low energy muon, for example, could not contaminate the considered sample of τ' events. Although one might relax the stringency of this cut to the criterion that the combined length of the apparently scattered K^+ track and the pion track be less than 5 cm, such a decision would clearly lead to an energy bias of the τ' spectrum. Furthermore, if a π^+ was seen to suffer an interaction (other than multiple scattering) between the K^+ and π^+ decay vertices, the event was rejected because: (1) it was impossible to learn whether or not the interaction were perfectly elastic; and (2) for a short range π^+ it was impossible to distinguish the true K^+ decay vertex from the π^+ scatter vertex. The events covered in objection (2) had been cut already by the exclusion of possible K^+ scatters within 5 cm of the apparent decay vertex. Each event was reviewed by an experienced scanner to ensure the correct interpretation of events accepted during the initial scan.

A shortcoming of the bubble chamber portion of the experiment was the inability always to detect the μ -kink in the $\pi^+ \rightarrow \mu^+ \rightarrow e^+$ chain. Since an accurate determination of the τ' to τ branching ratio would be required both for data analysis and possibly for matching the emulsion spectrum to the bubble chamber spectrum, it was necessary to ascertain the efficiency for detection of μ -kinks in order to apply an appropriate

THIS PAGE
WAS INTENTIONALLY
LEFT BLANK

correction factor. To this end a subexperiment was conducted to determine the μ -kink detection efficiency of the experienced scanners who ultimately reviewed all τ' candidates and passed judgment on the presence or absence of a μ -kink. The resulting efficiency factors, which were energy independent over the bubble chamber portion of the spectrum, were applied to the appropriate τ' samples uniformly over that energy range.

The scanning efficiency was determined separately for each of two categories of film. One class was characterized by an initial scan performed by several relatively inexperienced scanners; all rolls of this class were rescanned. The other class consisted of rolls scanned initially by experienced scanners with records of consistent scanning efficiencies; roughly $\frac{1}{4}$ of these rolls were rescanned. For both classes it was found that the average scanning efficiency for events remaining after fiducial volume and other cuts, which are described below, ranged from 80% to 90% for one scan. Hence the resultant efficiency for two scans ranged from 96% to 99%. The scanning efficiency was not energy independent: A maximum of 91% for a single scan was attained near the center of the energy range, from which the efficiency dropped monotonically to 89% at the lower end and to 77% at the upper end. The spectrum was adjusted so as to remove this energy dependence, dividing the number of events in each bin by the (fitted) efficiency for that bin. All accepted τ' events were measured on this campus, but the track fitting, determination of vertex location and of energy and angles, and tabulation of events were

accomplished with existing programs on the Berkeley IBM 7094 computer. Further data reduction and analysis were conducted with the IBM 7040 computer on the Riverside campus.

In order to obtain an odd-pion spectrum free of bias it was necessary to make several cuts in, and corrections to, the basic sample of events. First of all, a fiducial volume was defined so that a τ' event within the volume would have its μ -kink inside the bubble chamber, with the exception of the vertical direction. The effective fiducial volume was increased by extending the vertical coordinate to within 5 cm of chamber top and bottom and then weighting each event in this extended region by the ratio of the total solid angle to the solid angle lying within the chamber for the spherical surface generated by a radius vector of that pion's range and centered at the observed vertex. Both numerator and denominator of the ratio were corrected for dip angle cuts.

Range and dip angle cuts were jointly chosen to exclude all pion tracks with a range less than 12 mm and a dip angle from the horizontal plane greater than 60° , so as to ensure that a minimum projected track length would be greater than 6 mm and hence clearly visible.

The difficulty of distinguishing small azimuthal angle events for cases in which the ionization density was not much different for the stopping K^+ and the π^+ tracks of a τ' event forced azimuthal angle cuts, uniform over the odd-pion spectrum to avoid a bias, of $\pm 24^\circ$ from the forward direction and of $\pm 8^\circ$ from the backward direction. Following these cuts the sample

of events was checked for overall angular isotropy (exclusive of the cut intervals) with satisfactorily positive results.

Two corrections were made for the purpose of replacing events which had necessarily been rejected during data collection or cut during preliminary analysis. The first calculated correction was applied to the spectrum to account for the π^+ decays in flight between the two vertices. The second such correction returned to the sample events in which the π^+ track suffered a nuclear interaction enroute to its decay vertex. Treatment of K^+ decays in flight posed quite another problem. The scanning criteria imposed for recognition of a stopping K^+ track were that the primary K^+ track have very few gaps in its last 4 cm and no gaps of 1 mm or more in its last 1 cm. Furthermore, if a K^+ track formed an angle of more than 30° with the horizontal plane, that event was excluded because the projected ionization density of a dipping decay in flight might have been accepted as a stopping K^+ track. These criteria were based on the preliminary estimate that their use would permit scanners to identify and hence eliminate all K^+ decays with momenta greater than 200 MeV/c. A Monte Carlo calculation, based on this assumption and on the measured τ^+ spectrum, was then made to eliminate the remaining K^+ decays in flight (with K^+ momenta < 200 MeV/c) from the final τ^+ spectrum. The correction was then adjusted so as to contain the same cuts as those imposed on the experimental data. This problem of K^+ decays in flight will be studied further by means of the τ events, where a decay in

flight is kinematically obvious beyond the uncertainties introduced by measurement error and range straggling. Another subtractational correction was made, based on a Monte Carlo calculation, to remove $K_{\pi 2}^+$ decays in flight with the π^+ track in the backward hemisphere.

Percentages of the total sample lost through the various cuts are listed in Table I, whereas the numbers of events restored to the individual bins of the spectrum through calculated corrections are displayed in Table II.

2. τ Data

The τ mode of K decay was recognized by the distinctive set of three charged pion tracks emanating from the vertex. So prominent were these events that the average scanning efficiency was about 90% on a single scan. As a consequence barely two-fifths of the film was rescanned for this type of event.

Several cuts and corrections were needed for this mode, too, in order to obtain an odd-pion spectrum free of bias. Near stopping K^+ decays in flight, however, were detected within the uncertainties of measurement error and range straggling with a kinematics check during computer processing and hence posed no serious problem. Events possessed of at least one π^+ track which suffered an interaction enroute to its decay vertex were excluded from the measured sample, as in the τ' case. The additive corrections for π^+ decays in flight and the π^+ nuclear interactions were also applied to τ events.

Despite the clear signature of the τ mode, there were a large number of events identified in scanning which could not

be located exactly in at least two (of the three) views. Especially in the case of a very short pion track it was sometimes impossible to determine the origin and terminus with accuracy sufficient for measurement. Exclusion of these events would bias the odd-pion energy spectrum so the supplementary data from emulsion will be required for the ultimate τ data fitting.

Table I

Cause of Loss	Percent of Total Sample Lost
Fiducial Volume	16.6
π^+ Dip	9.5
K^+ Dip	8.8
Azimuth Angle Difference	9.6
π^+ Scatter	5.2
K^+ Scatter in 5 cm before VTX	6.0
Muon Class 1	16.3

B. Emulsion Scanning and Measurement

The stack from which the K^+ decays used in the present investigation were obtained is that previously used at UCRL for a determination of the K^+ decay branching ratios. The stack consists of 250 pellicles of Ilford K5 emulsion pellicles each of dimensions 9" x 14" x 600 μ .

The area in each of 19 plates where the density of K^+ track endings was greatest was scanned specifically for τ^+ candidates and τ decay events. An event was accepted for a τ^+

candidate if there was a single secondary (decay) track which contained more than 38 grains in the first 125 μ of track (corresponding to $g^* \sim 1.5$). This criterion excluded $K_{\mu 2}$, $K_{\pi 2}$, $K_{e 3}$ and the higher μ^+ energy $K_{\mu 3}$ modes. In addition, the τ' events in which the π^+ had near maximum energy are excluded. However, since the object of this section of the experiment was to concentrate on the lower part of the π^+ spectrum it will be seen that the loss of these τ' decays was unimportant. A dip criterion was also imposed during scanning. The secondary was required not to dip more than 50 μ for 100 μ projected length (corresponding to an original angle of $\sim 45^\circ$). The grid positions of the accepted τ' candidates and the observed τ decays were noted down. It was also noted whether the decay took place within 50 μ of either surface of the pellicle.

For the purpose of estimating scanning efficiencies each plate was completely rescanned by a different scanner using the identical criteria as before.

The secondary track from each of the τ' candidates was followed through successive pellicles until it either stopped or until 1 cm of track had been followed. (The estimation of this range was made using a simple-constructed analog computer.) Since it was known from previous data that the detectability of π^+ mesons from K^+ decays began to drop for energies greater than about 20 MeV, this energy was chosen as an upper limit in this investigation. (A 1 cm π^+ has an initial energy of ~ 22 MeV.) The application of this range cut-off enabled the work to proceed at a faster pace.

If the secondary track stopped, it could be identified easily as a π^+ by the distinctive $600 \mu \mu^+$ track. Consequently the contamination from $K_{\mu 3}$ decays was eliminated.

The ranges of the π^+ from the accepted τ' decays were measured using a digitized microscope, and hence the energies were calculated.

The scanning efficiencies were calculated for various energy intervals and it was found that there was no evidence for an energy-dependent scanning efficiency. The overall scanning efficiencies in the first and second scans are $(71.0 \pm 1.8)\%$ and $(83.3 \pm 1.6)\%$ respectively. A total of 756 events have been found. A maximum likelihood estimate of the true number of events present is 794 and there is 90% confidence that there are no more than 805.

In the same volume of emulsion 6360 τ decays have been found. The efficiencies for the 1st and 2nd scans are $(89.9 \pm 0.4)\%$ and $(89.2 \pm 0.4)\%$ respectively. The estimate of the true number of τ decays present is 6430. This, together with the latest estimate of the τ branching ratio $(5.6 \pm 0.1)\%$ indicates that the τ' decays from which the spectrum is to be assembled are an exclusive portion of the decay of about 165,000 K^+ mesons. (The geometrical dip-cut factor has been included.)

In connection with this program a detailed study of scanning efficiencies led to an improved theory of efficiency measurement. This work has been reported:
David A. Evans and Walter H. Barkas, "Exact Treatment of Search Statistics" UCR P107-42. Submitted to the Physical Review.

Another by-product of this work was the paper:

Walter H. Barkas, "Velocity Determination in Bubble Chambers"
UCR P107-36, published in Review of Scientific Instruments 38,
425 (1967).

III. Preliminary Results

Because of the rather large number of cuts and corrections which the τ data require it is not yet in final form. Tests for isotropy have yet to be completed. When only crude energy independent cuts are made, much data is wasted, and we shall attempt to make better use of the data by making energy dependent cuts and corrections.

Among the factors we are considering are corrections for contaminations, decays in flight, π^+ and K^+ scattering effects, scanning efficiencies as function of energy and dip angle.

The rather heavily cut bubble chamber data are presented in Fig. I. The similar emulsion data are shown in Fig. II. The τ data has not yet been carried to this stage.

References For Three-Pion Decay

1. W. A. Dunn and R. Ramachandran, Phys. Rev. 153, 1558 (1967).
2. S. Weinberg, Phys. Rev. Letters 4, 87 (1960); and 4, 585E (1960).
3. P. Budini and L. Fonda, Phys. Rev. Letters 6, 419 (1961).
4. A. Callahan et. al., Phys. Rev. 150, 1153 (1966).
5. G. Kalmus et. al., Phys. Rev. Letters 13, 99 (1964).
6. G. Alexander et. al., Nuovo Cimento 6, 478 (1957).
7. G. Harris et. al., Roch. Conf. Proc. VIII-26 (1957).

8. B. Bhowmik et. al., Nuovo Cimento 8, 147 (1958).
9. S. Taylor et. al., Physical Review 114, 359 (1959).
10. J. Boggild et. al., Nuovo Cimento 19, 621 (1961).
11. G. Giacomelli et. al., Phys. Letters 3, 346 (1963).
12. V. Bisi et. al., Nuovo Cimento 35, 768 (1965).
13. S. Fung et. al., Proc Inst. Conf. on H.E.P., Berkeley (Sept. 1966).
14. S. Taylor et. al., Nuclear Phys. 83, 690 (1966).
15. Brown and Singer, Phys. Rev. 133, B812 (1964).
16. A. Mitra and Ray, Phys. Rev. 135, B146 (1964).
17. G. H. Trilling, in Proceedings of the International Conf. on Weak Interactions (Argonne National Laboratory, Chicago (1965)). p. 115.
18. Henry D. I. Abarbanel, Phys. Rev. 153, 1547 (1967).
19. N. N. Khuri and S. B. Treiman, Phys. Rev. 119, 1115 (1960).
20. R. W. Birge, R. P. Ely, G. Gidal, G. E. Kalmus, A. Kerman, W. M. Powell, U. Camerini, D. Cline, W. F. Fry, J. G. Gaidos, D. Murphee, and C. T. Murphy, Phys. Rev. 139, B1600 (1965).
21. G. Källén, "Elementary Particle Physics", Addison-Wesley, Palo Alto, 1964.
22. T. D. Lee and C. S. Wu, "Weak Interactions", Annual Review of Nuclear Science 16, 471 (1966).
23. Walter H. Darkas, "Masses of the Metastable Particles", Annual Review of Nuclear Science 15, (1965).
24. I. M. Barbour and R. L. Schult, "Faddeev Equations for the $K \rightarrow 3\pi$ Amplitude", Phys. Rev. 155, 1712 (1967).

TABLE II

<u>Bin (MeV)</u>	<u>Basic Events in Bin</u>	<u>Correctional Additions</u>	<u>Final Events in Bin</u>
14 - 16	201	20	221
16 - 18	179	16	195
18 - 20	189	19	208
20 - 22	162	16	178
22 - 24	186	19	205
24 - 26	186	20	206
26 - 28	190	22	212
28 - 30	172	21	193
30 - 32	142	20	162
32 - 34	144	21	165
34 - 36	150	24	174
36 - 38	101	18	119
38 - 40	85	17	102
40 - 42	87	18	105
42 - 44	79	19	98
44 - 46	67	16	83
46 - 48	53	16	69
48 - 50	44	15	59
50 - 52	31	9	40

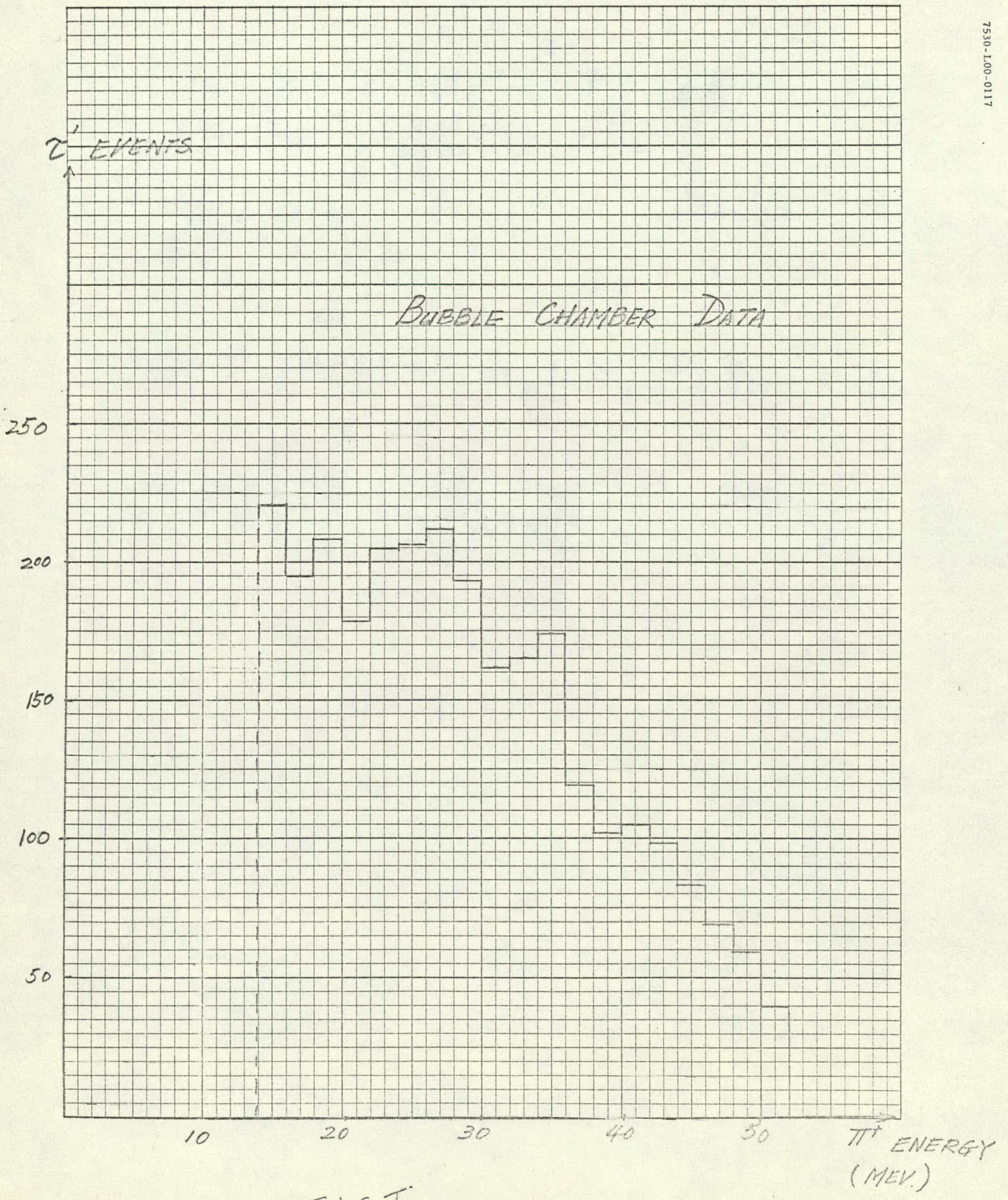


FIG I



τ EVENTS

50

EMULSION DATA

25

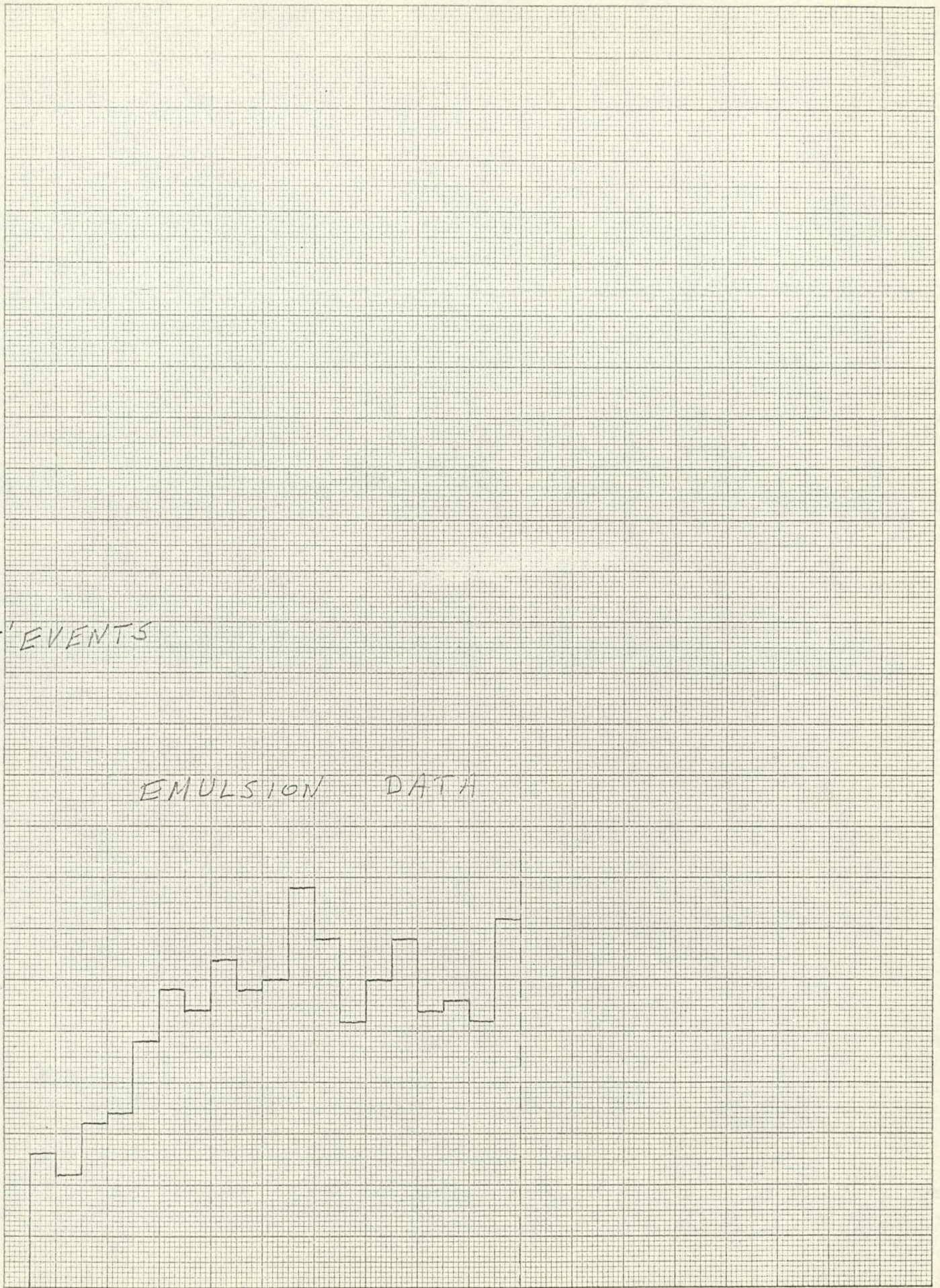
0

10

20

π^+ ENERGY (MeV)

FIG. II



Program B - Hypernucleus Studies

Heh Zhang, David A. Evans and W. H. Barkas

An investigation is in progress of the hypernuclei produced in the captures of K^- mesons by nuclei in emulsion. The emulsion stack being used is one exposed at Berkeley and previously partially scanned there. Some additional scanning, specifically for hypernuclei, has been undertaken here.

The total number of hypernuclei found at present is 326 of which 50 decay mesonically (i.e. with the emission of a charged π).

The primary stars (viz. those in which the hypernuclei are produced) have been classified in the usual way, and N_D , N_L distributions etc. have been compiled. The range distribution of the hypernuclei has also been obtained.

An attempt is being made to identify the hypernuclei which decay mesonically. To achieve this, a kinematic analysis of the decay is tried. The ranges and space angles of the charged decay products are obtained from measurements on the tracks. In general, however, the identities of these particles are unknown (except for the π). Each such track is assigned in turn all nuclear identities from a proton to, for example, O^{19} . All possible permutations are constructed for the various track identities. For each permutation such kinematical quantities as momentum unbalance (the hypernuclei decay at rest), energy release and Λ binding energy are calculated. Those permutations with not unreasonable values for these quantities are then

examined closely and an attempt made to choose the best one. Hence the identity of the hypernucleus may be deduced. In general, such unique identification is rare and there is usually some ambiguity. However, fairly close limits on the charge and mass of the hypernucleus may be set.

Clearly, these calculations require the use of a computer. We have obtained from CERN a program which performs essentially as described, with several refinements. This program has been modified here to run on the IBM 7040 available on the campus.

Due to lack of man power, the measurement of the decays has progressed only slowly. The range of the π is frequently of the order of 1.5 cm which involves following the track through several plates. The measurement of these long tracks is done using a digitized microscope. The ranges of the shorter tracks are obtained from the eyepiece reticle. This information together with the azimuths and dips of the tracks is punched into cards as input for the identifying program. It is expected that by the end of the summer all the mesonic hypernuclei will have been measured and put through the program.

In connection with the program the following paper was written: Cliff Fok and Walter H. Barkas, "The Pion Range Energy Curve in The Region Useful for Mesonic Decay of Hypernuclei" UCR P107-38, published in Nuovo Cimento 48A, 587 (1967).

Program C - High Energy π^+ Interactions

R. B. Bacastow, S.-Y. Fung, W. Jackson and R. T. Pu

A π^+p experiment has been underway during the past year. This is a collaborative effort with the Powell-Birge group of the Lawrence Radiation Laboratory at Berkeley. The Berkeley 72 in. hydrogen bubble chamber was exposed to pion beams at five incident momenta: 2.9, 3.3, 3.5, 3.7 and 4.0 GeV/c. This corresponds to a center-of-mass energy range of roughly 2.5 - 2.90 GeV. A total of about 200 rolls or 150,000 pictures were distributed among these five momenta.

The primary purpose of this experiment is to study the various multiparticle reactions in general and in particular the quasi-two-body reactions such as $\pi^+p \rightarrow \rho^0 N^{*++}$ and $\pi^+p \rightarrow \omega N^{*++}$. The experiment will afford a detailed study of the energy dependence of the various reaction channels in this energy range. Increased statistics in this experiment over previous experiments in this energy range will afford a better comparison with theoretical models. Of particular interest is the investigation of evidence for the reported resonance $N^*(2830)$ in various reaction channels. In the following we briefly describe the several areas where major effort has been placed.

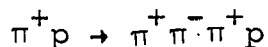
A. Beam Normalization

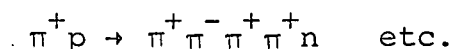
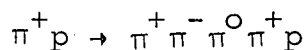
To study the energy variation of the several reaction channels, e.g. the energy variation of the total cross section in a given channel, an accurate beam normalization is essential. The problem is to find the number of pions entering the chamber

along with a contamination of protons and muons. Several ways and means have been explored. The most promising method and the one finally pursued is δ -ray production. Briefly, for a given incident momentum, light particles make higher energy δ -rays than heavier particles. Thus by counting only energetic δ -rays, one effectively separates the protons in the beam from the pions and muons. In addition, the number of secondary interactions (a strong interaction on a track after a large δ -ray) effectively separates non-interacting μ 's from the π 's. In this experiment, δ -rays with radius larger than $\sim 7/8$ " on the scanning table have been recorded. This corresponds to a δ -ray energy of about 18 MeV. Care has been taken in selecting beam tracks by their incident angle, position in the beam window, track curvature, etc. Various self-consistency checks were performed in each stage. Since the δ -ray production cross section is well known theoretically, an absolute π^+ beam normalization can be obtained. To assure uniformity and good statistics, alternating rolls in each energy have been δ -ray scanned and measured. The final result of $\Delta \pi^+$ ^{the average number of} beam tracks/picture is obtained with about 1.5% statistical accuracy at each energy.

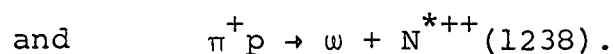
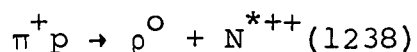
B. Four-Prong Events

All four-prong events, a total of about 40,000, were rough digitized and then accurately measured on the automatic measuring machine FSD, at the Lawrence Radiation Laboratory. These events are fitted to reactions such as





Prime attention was given to the p dominant quasi two-body reaction channels



Preliminary data was reported in a post-deadline paper at the APS Washington D. C. Meeting in April, 1967. (UCR P107-48).

Increased statistics and greatly extended range in the momentum transfer distribution ($\frac{d\sigma}{dt}$) over previous data¹ shows in the $\rho^0 N^{*++}$ reaction a "dip" behavior near $t = -0.4$ similar to that observed in $\pi^\pm p$ elastic scattering. Spin density matrix elements computed from the preliminary data are being compared with theoretical predictions. In certain respects, particularly in the ρN^* reaction the data deviates from the spherical absorption model calculation of Jackson et. al.² An attempt is being made to see if the observed data can be explained by a combination of a π^0 exchange amplitude with absorption in the t-channel, and an S-channel resonance of the $N^* (2830)$ decaying into ρ and $N^* (1238)$ final states. A good fit of this hypothesis to the observed spin density matrix elements could constitute a powerful tool in the determination of the J^P value of the $N^* (2830)$.

C. $\pi^+ p$ Backward Elastic Scattering

A backward elastic scattering peak in high energy $\pi^+ p$.

scattering has been observed recently.³ We have looked for π^+p backward elastic events in our film since the backward peak may also yield important information concerning the J^P values of the N^* (2830) resonance. We scanned for candidate events in which one pion-like track scattered more than 45° from the incident direction with another forward scattered fast proton track within the forward cone of 25° . This corresponds roughly to the geometry of backward scattering in the center of mass frame at angles larger than 120° . About 40 candidate events/roll were obtained. However, on the average only about 0.5 events per roll passed the kinematic fitting program for π^+p backward elastic scattering. This is less than half the number of events we would expect from previous experimental data. This low yield may be due to statistical fluctuation. A combined plot does show a backward peak with a dip similar to previous experiments. Unfortunately the low statistics makes further detailed analysis very difficult. For those events fitting the reactions $\pi^+p \rightarrow \pi^+p\pi^0$ with the pion backward, the invariant mass plot of the $p\pi^0$ combination reveals a peak near 1700 MeV. This may indicate decay of the N^* (2840) into N^* (1688). Further study in this is in progress.

References For High Energy π^+ Interactions

1. G. Goldhaber et. al., Phys. Letters 18, 76 (1965); S. Goldhaber et. al., Phys. Rev. Letters 15, 737 (1965).
2. J. D. Jackson et. al., Phys. Rev. 139, B428 (1965); J. D. Jackson and H. Pilkuhn, Nuovo Cimento 33, 906 (1964); 34, 1841E (1964).
3. C. T. Coffin et. al., Phys. Rev. Letters 15, 838 (1965); H. Brody et. al., Phys. Rev. Letters 16, 828 (1966).

Program D - K^- - p Interactions

W. H. Barkas, R. B. Bacastow, S.-Y. Fung,

E. L. Hart and R. T. Pu

Only planning work has been carried out on this project.

Program E - Electromagnetic Processes Induced by High Energy
Electrons

Arthur Cary, D. A. Evans and W. H. Barkas

An experiment is being carried out on the inelastic electron interactions in nuclear research emulsion. We are determining cross sections for electron-nuclear interactions and electron pair production, and are looking for possible anomalies that might exist in electromagnetic interactions at high energies.

Ten Ilford G5 emulsions about 12.5 cm long and 2.5 cm wide and 600 μ thick were exposed perpendicularly to the SLAC electron beam at beam energies of 16 GeV, 10 GeV, and 5 GeV. During the same experiment 200 μ emulsion were exposed parallel to the beam to investigate electron pair production. It was initially anticipated that the electron beam intensity would be 10^7 - 10^8 /cm²; preliminary measurements indicate an intensity of $\sim 10^7$. All of the emulsions exposed perpendicularly had a 1 mm grid printed on their bottom to facilitate recording and relocation of events.

At present the major scanning effort is being applied to emulsion exposed perpendicular to the 16 GeV beam. When all the emulsions have been examined an effective track length of 7.5×10^6 cm will have been viewed. Assuming a cross section of the order of magnitude of that determined by George and Evans, and Kile et. al. for stars produced by muons ($\sim 10^{-30}$ /cm²), we estimate an interaction length of about 2×10^3 m. This indicates we should expect about 35 stars with 3 or more prongs per plate and about 150 single pronged interactions per plate.

A major existing problem is ^{to} establish a satisfactory set of criteria for separating electron produced stars from other stars that may have coincident electron tracks; the quality of the emulsion makes this difficult. The recording of single prong events may also increase the overall scanning time. To date about 5,000 stars of all kinds have been recorded; about 10% of these seem to have a coincident electron above the star. The incident electron flux is being measured with the use of a television camera and monitor, allowing an enlarged view of a reduced field of vision. It is expected that this technique will yield very accurate measurements of incident flux.

Those stars which seem to have an incident track must be rescanned and examined more closely to determine which are truly electron produced.

In connection with this program the following paper was written:

Walter H. Barkas, "Possible Roles for Emulsion As A Detector In Experiments With Future High Energy Accelerators" UCR P107-34, published in the Proceedings of the VI International Conference on Corpuscular Photography, Florence, Italy; July 19-23, 1966.

Program F - High Energy $\bar{p}p$ Scattering

E. L. Hart, T. Mellon and U. Mehtani

We have made a measurement of the cross section for 7 BeV/c antiproton-proton elastic scattering over the backward hemisphere, $90^\circ < \theta_{cm} < 180^\circ$, a range of $-t$ from 5.7 to 11.4. A backward peak in both π^+p and π^-p elastic scattering has been observed^{1,2,3} over a wide range of incident pion momenta up to 8 BeV/c. The existence and dependence on s (square of the cm energy) and t (square of the four-momentum transfer) of these peaks is consistent with the Regge-pole theory^{4,5} for $N(I = \frac{1}{2})$ and $\Delta(I = \frac{3}{2})$ exchange. Some of the features are also consistent with the "coherent droplet" model of Byers and Yang.⁶

Several bubble chamber groups have studied $\bar{p}p$ elastic scattering at 7.0,⁷ 5.7,⁸ 4,⁹ 3.3 and 3.7,¹⁰ and 3.6 and 3.0¹¹ BeV/c. Only in the 3.0 BeV/c experiment were the statistics sufficient to observe elastic scattering in the backward hemisphere. A plot of $\log \frac{d\sigma}{dt}$ vs $-t$ for $\theta_{cm} > 90^\circ$ appears, at 3.0 BeV/c, to have the \sim constant slope that is observed for $-t > 1.0$ in all the experiments. There is no evidence of a backward peak. Elastic $p-p$ scattering can only be observed to $\theta_{cm} = 90^\circ$.

For this study, approximately 10,000 pictures from the BNL 80" hydrogen bubble chamber yielded 1.25×10^7 cm of track in the fiducial region. The beam purity is known to be $95 \pm 1\%$, and the momentum $6940 \text{ MeV/c} \pm 2\%$ with a spread of $\pm 5\%$.⁷ A total of 9202 two-prong events were observed. Of these, 111 satisfied the scanning criteria; a) outgoing tracks lie on opposite

sides of the beam track, b) positive outgoing track not more dense than the negative outgoing one, c) positive track's projected emission angle not greater than that of the negative track, d) radius of curvature of positive track not smaller than that of the negative track. A second scan of 40% of the film yielded a joint scanning + selection efficiency of 87%. The efficiency for observing backward elastic scattering in the range $-t = 11.3$ to 11.4 , $\theta_{cm} = 168^\circ - 180^\circ$, is higher, as the antiproton will stop in the chamber and annihilate, giving a high probability of a star associated with the scattering. No such event was observed.

The successful candidates were measured and fitted with the Berkeley FOG-CLOUDY-FAIR system. Only one, $\theta_{cm} = 91 \pm 0.5^\circ$, made a successful fit to an elastic event. A sample of 50 forward scattering events were measured, of which 18 made unambiguous elastic fits.

An extrapolation of the results of the 5.7^8 and 7.0^7 BeV/c experiments permits an estimate of the cross section to be expected over the backward hemisphere, assuming no backwards peak. The 7.0 BeV/c measurements of elastic scattering extend to $\theta_{cm} = 33^\circ$, $-t = .8$, so no slope can be obtained for $\log \frac{d\sigma}{dt}$ vs $-t$ at $-t > 1.0$. However, the other experiments indicate that the slope is independent of the incident momentum. Taking the 5.7 BeV/c results for the slope, and the 7 BeV/c for $(\frac{d\sigma}{dt})_{t=0}$, the expected cross section is $\sim 1.2 \mu b$, compared with the observed $2.5^{+3.4}_{-1.8} \mu b$.

The π^+ -p and π^- -p backward peaks for all incident energies appear to be contained in the region $|t_{\max}| \sim .7$ to $|t_{\max}|$. No \bar{p} -p elastic events have been observed in this region, giving a cross section $< 2.4 \mu\text{b}$. For $Q_{\pi\text{-p}} = Q_{\bar{p}\text{-p}}$, the π^+ -p and π^- -p cross sections, integrated over the region of the backward peak are approximately 14.5 and 3.4 μb respectively. The probability of not observing an event, if there is a \bar{p} -p backward peak as large as the π^+ -p, is .0024. For the π^- -p peak the probability is .242.

Applying the Regge-pole argument, \bar{p} -p backward elastic scattering involves the exchange of a deuteron trajectory as for the N and Δ trajectories, the magnitude of $\frac{d\sigma}{dt}$ at a given t in the vicinity of t_{\max} should fall as $1/s^8$ compared with $1/s^3$ for π^+ -p. Since one should expect the π , p couplings to the N and Δ are roughly the same as the p,p coupling to the D, a backward peak in \bar{p} -p elastic scattering should be several orders of magnitude smaller than the corresponding π -p cross section, and unobservable here.

In the Byers-Yang model, backward scattering does not require large momentum transfers, or the exchange of a massive particle, but rather the transfer of quantum numbers, i.e., nucleon number in this case. The \bar{p} -p backward cross section would then be expected to be of the same order of magnitude as the π -p, or any other two particle cross sections; this is not observed here.

We wish to thank Dr. M. Webster of the BNL Bubble Chamber Group for the use of the film, and Dr. H. White for the use of his programs and computer. We are grateful to Dr. N. Byers, Dr. B. Desai, and Dr. G. B. Yodh for helpful discussions.

References For High Energy $\bar{p}p$ Scattering

1. W. R. Friskin, A. L. Read, H. Ruderman, A. D. Krisch, J. Orear, R. Rubinstein, D. B. Scarl, and D. H. White, Phys. Rev. Letters 15, 313 (1965).
2. C. T. Coffin, N. Dikmen, L. Ettliger, D. Meyer, A. Saulys, K. Terwilliger, and D. Williams, Phys. Rev. Letters 15, 838 (1965).
3. H. Brody, R. Lanza, R. Marshall, J. Wiedner, W. Selove, M. Shochet, and R. Van Berg, Phys. Rev. Letters 16, 828 (1966).
4. C. B. Chiu and J. D. Stack, Phys. Rev. 153, 1575 (1967).
5. S. C. Frautschi, Regge Poles and S-Matrix Theory (W. A. Benjamin, Inc., New York, 1963).
6. N. Byers and C. N. Yang, Phys. Rev. 142, 976 (1966).
7. J. A. Johnson III, Thesis, Yale University (1965).
8. K. Böckmann, B. Mellen, E. Paul, B. Wagini, I. Borelka, J. Diaz, U. Heeres, U. Liebermeister, E. Lohrmann, E. Raubold, P. Söding, S. Wolff, J. Kidd, L. Mandelli, L. Mosca, V. Pelosi, S. Ratti, and L. Tallone, Nuovo Cimento 42, 954 (1966).
9. O. Czyzewski, B. Escoubes, Y. Goldschmidt-Clermont, M. Guinea-Moorhead, D. R. O. Morrison, and S. De Unamino-Escoubes, Physics Letters 15, 188 (1965).
10. T. Ferbel, A. Firestone, J. Sandweiss, H. D. Taft, M. Gailloud, T. W. Morris, A. H. Bachmann, P. Baumel, and R. M. Lea, Phys. Rev. 137, B1250 (1965).
11. B. Escoubes, A. Fedrighini, Y. Goldschmidt-Clermont,

M. Guinea-Moorhead, T. Hofmohl, R. Lewisch, D. R. O. Morrison, M. Schnellberger, and S. De Unamino, Physics Letters 5, 132 (1963).

12. $Q = E^* - M_3 - M_4$, E^* = total energy in the cm system, and M_3 and M_4 are the masses of the two outgoing particles. In comparing cross sections of equal and unequal mass particles, we assume that the most reasonable parameter is the available energy in the cm system, although it is not one of the parameters of the Regge-pole equations. S. Meshkov, G. A. Snow, and G. B. Yodh, Phys. Rev. Letters 12, 87 (1964).
G. B. Yodh, private communication.

UCR P107-48

Post Deadline paper submitted to the American Physical Society Meeting, Washington D. C., April 1967.

Abstract

The Quasi-Two Body Reactions $\pi^+p \rightarrow N^{*++}(1238)\rho^0$
 $\pi^+p \rightarrow N^{*++}(1238)\omega^0$. Between 3 and 4 GeV/c. D. Brown, G. Gidal, Lawrence Radiation Laboratory, Berkeley; R. B. Bacastow, S.-Y. Fung, W. Jackson and R. T. Pu, University of California, Riverside. Differential Cross Sections and density matrix elements are presented for the reactions $\pi^+p \rightarrow N^{*++}(1238)\rho^0$ and $N^{*++}(1238)\omega^0$ based on analysis of 40,000 four-prong events distributed among 5 energies between 3 and 5 GeV/c. The momentum transfer distribution for the $N^{*++}(1238)\rho^0$ reaction shows a "dip" behavior near $t = -0.4$ similar to that observed in π^+p elastic scattering. The $N^{*++}(1238)\omega^0$ reaction is compared to the reaction $\pi^-p \rightarrow N^{*++}(1238)\pi^-\pi^-$.

Publications

Copies of the following reports are attached.

1. D. Brown, G. Gidal, R. Bacastow, S.-Y. Fung, W. Jackson, and R. Pu, "The Quasi-Two Body Reactions $\pi^+ p \rightarrow N^{*++} \rho^0$ and $\pi^+ p \rightarrow N^{*++} \omega^0$, (UCR P107-48).
2. Walter H. Barkas, "Velocity Determination in Bubble Chambers", (UCR P107-36), published in Rev. Sci. Inst. 38, 425 (1967).
3. David A. Evans and Walter H. Barkas, "Exact Treatment of Search Statistics", (UCR P107-42), submitted to Physical Review.
4. Cliff Fok and Walter H. Barkas, "The Pion Range-Energy Curve in the Region Useful for Mesonic Decay of Hypernuclei", (UCR P107-38), published in Nuovo Cimento 48A, 587 (1967).
5. Walter H. Barkas, "Possible Roles for Emulsion as a Detector in Experiments With Future High Energy Accelerators", (UCR P107-34), for publication in Proceedings of VI International Conference on Corpuscular Photography.

Velocity Determination in Bubble Chambers*

WALTER H. BARKAS

University of California, Riverside, California 92502

(Received 27 October 1966; and in final form, 28 November 1966)

The kind of information that can be obtained from a bubble chamber track is analyzed and the statistical reliability of each parameter is given. Practical matters entering into the measurements are discussed.

AT the 1966 International Conference on Instrumentation for High Energy Physics, there was general agreement (as there was not at earlier meetings) that a need exists for the velocity estimates that can be derived from bubble density measurements. However, a lack of understanding seems to prevail regarding known aspects of the subject. This paper assembles the results of detailed studies of several years ago that remain applicable.

A unit length of track contains an average number g_0 of points at which bubbles begin to grow when the chamber is expanded. These are the sites of "thermal spikes," which occur at the termini of delta rays¹ or elsewhere when energy of more than a few hundred electron volts is deposited in a very small volume. Now $g_0 = ze^2 C(P, T) f(\beta)$, where ze is the charge carried by the particle making the track, $C(P, T)$ is a characteristic function of pressure, P , and temperature, T , of the bubble chamber liquid, and $f(\beta) \approx \beta^{-n}$ (with $n \approx \text{constant} \approx 2$ for hydrogen) over a wide range of the particle velocity, β .¹⁻⁷ One attempts to optimize the pressure and temperature of the liquid and to

keep them constant in time and space, but as chambers become larger, maintaining constancy becomes difficult. In order to determine the particle velocity from a measured g_0 , the functions $C(P, T)$ and $f(\beta)$ must be known. They can be obtained best by calibration using particles of known velocity.

In unit length of track as seen projected on a plane which is normal to the line of sight, an average number $g (= g_0 \sec \delta)$ of bubble sites is present. Here $\pi/2 - \delta$ is the angle between the track segment and the normal to the plane.² If δ exceeds 30° or so, numerous problems are encountered, but the structure of an inclined track with an apparent bubble density g , measured in the projected image of the track, is the same as that of a track lying in the plane with true bubble density g_0 .

Bubble sites are produced at random along the particle path, and the number of bubbles present in a track segment is all the information regarding the particle velocity that is obtainable from it. When the bubbles are mere points and are completely resolvable, g has the standard deviation σ_g of a Poisson distribution

$$\sigma_g = g/\sqrt{N}, \quad (1)$$

where N is the number of bubbles in the available segment of track. This estimate is the minimum possible standard deviation of g . Actually, the bubbles grow after the chamber is expanded and perfect optical resolution is unattainable. All the bubbles thus are not resolved on the film so as to be countable. The linear structure of the track really consists of unresolved clumps or "blobs" of bubbles alternating

* This work was supported by the U. S. Atomic Energy Commission Contract No. AT(11-1)34 P107B.

¹ D. V. Bugg, *Progress in Nuclear Physics* (Butterworth-Springer, London, 1959).

² W. H. Barkas, *Phys. Rev.* **124**, 897 (1961).

³ W. J. Willis, E. C. Fowler, and D. C. Rahm, *Phys. Rev.* **108**, 1046 (1957).

⁴ G. A. Blinov, I. S. Krestnikov, and M. F. Lomanov, *Soviet Phys. —JETP* **4**, 661 (1957).

⁵ V. P. Kenney, *Phys. Rev.* **119**, 432 (1960).

⁶ A. Ahmadzadeh and N. N. Biswas, *Nuovo Cimento* **19**, 958 (1961).

⁷ C. Dilworth, D. R. O. Morrison, and G. Mernbriani, *Nuovo Cimento* **32**, 1432 (1964).

with "gaps." Not N but N' blobs are present in the track segment, a fraction L of which consists of gaps.

Because the edge of a bubble is poorly defined optically, a minimum gap length ϵ often has been introduced. This is equivalent to increasing the bubble diameter by the length ϵ . Dilworth *et al.*⁷ estimated that to find a strictly exponential gap length distribution, one might have to take ϵ equal to one-half the bubble diameter, [see Eq. (2)]. The question remains moot whether or not ϵ can be reduced to zero by introducing objective criteria defining the bubble-gap boundary; the writer believes this to be possible. To avoid argument and obtain objective results, however, one can simply require that the length l of a gap be the apparent distance along the particle trajectory between two blobs reduced by the length ϵ . The length b of a blob similarly is its apparent length increased by ϵ .

Both observation³⁻⁷ and theory⁸ then show that the distribution of gap lengths is exponential, so that the density of gaps $H(l)$ exceeding length l is given by

$$H = B \exp(-gl). \quad (2)$$

Here B is the blob or gap density. It is related to g by the formula $B = g e^{-\alpha g}$, where α is a parameter discussed below. The observed B does not have a Poisson distribution, but has a lower variance given by

$$\sigma_B^2 = (B^2/N')[1 + 2L \ln L]. \quad (3)$$

From the form of H , $g = 1/\bar{l}$, where \bar{l} is the mean gap length. This formula is correct regardless of what value of ϵ is required. If a large ϵ is used, information is lost, many small gaps go out of existence, and the average blob length \bar{b} increases, but the mean gap length remains unchanged. The expression $g = 1/\bar{l}$ is a statistically better estimate of g than the slope of the $\ln H$ vs l line.

The quantity α is a length, "the mean bubble diameter," determined by the choice of ϵ , the bubble size, and the optical resolution as measured on the film. All these effects are lumped in this single parameter.⁹ The definition of α ¹⁰ implies a very weak or no dependence on the energy-loss rate of the particle. The mean blob length \bar{b} is²

$$b = (e^{\alpha g} - 1)/g = \frac{1}{B} - \frac{1}{g}. \quad (4)$$

⁸ W. H. Barkas, *Nuclear Research Emulsions* (Academic Press Inc., New York, 1963).

⁹ Light coming to the film may have suffered chromatic dispersion. The bubble image then may be drawn out so that its image is not circular. In this case, α must be measured on tracks having the same direction as the test track. This effect may be eliminated by monochromatic illumination. Sometimes the bubbles are so illuminated that their images are mere crescents. Again test and comparison tracks should be parallel and adjacent. These complications admittedly make α less well-defined in the bubble chambers than in emulsion, but they may be largely overcome.

¹⁰ Ref. 8, formula 9.12.18. The development of this section applies with only minor changes to bubble tracks.

The quantity α is to be obtained from other tracks preferably of similar ionization. We define the "lacunarity," L , by

$$L = \bar{l}/(\bar{l} + \bar{b}) = e^{-\alpha g}. \quad (5)$$

This has a variance given by

$$\sigma_L^2 = 2L^2/N'[1 - L + L \ln L]. \quad (6)$$

Then a measure of α is²

$$\alpha = -(L/B) \ln L. \quad (7)$$

Assuming that α does not depend on ionization, another estimate of it is obtained by finding the maximum value of B , B_m , on any track. Then,² $\alpha = (e B_m)^{-1}$. At this point $\alpha g_m = 1$ and $B_m \bar{l} e = 1$. In these equations, e is the base of the natural logarithms.

The product $(\alpha + l)H(l)$ is a universal function of $(\alpha + l)g_0 \sec \delta$. Thus

$$(\alpha + l)H(l) = (\alpha + l)g_0 \sec \delta \exp[-(\alpha + l)g_0 \sec \delta]. \quad (8)$$

When α increases, information is lost. To augment the information content of track-segments, α may be decreased by improved optics and by photographing "younger" tracks. In addition, g can be increased by varying the expansion pressure-ratio and the initial temperature.

The information lost because α is not vanishingly small can be partially regained by measuring \bar{b} . This constitutes entirely new information, quite independent of the estimate of g from \bar{l} .

It has been shown² that \bar{l} and \bar{b} exhaust the information regarding g in the linear structure of the track. Whereas at small values of g , \bar{l} contains most of the particle velocity information, at high values of g a better estimate is obtained from \bar{b} . This value of g is best obtained from a graph of αg vs \bar{b}/α using Eq. (4). The formulas for B , L , \bar{b} , and \bar{l} , using data from a number of track segments, have been found to yield consistent estimates of g .¹¹

The values of g obtained from the measurements of \bar{l} and \bar{b} in a track segment can be combined as independent estimates. The standard deviation of g obtained from \bar{l} is $\sigma_g = g/\sqrt{N'}$, where N' is the number of gaps or blobs used for the measurement. The measurement of \bar{b} yields an estimate of g with a somewhat more complicated standard deviation. It is given by

$$\sigma_g = \frac{g[1 + L^2 + 2L \ln L]^{\frac{1}{2}}}{\sqrt{N'(L - \ln L - 1)}}, \quad (9)$$

if α has been determined independently (with negligible error) from measurements on similar tracks. The fractional error in g_0 is the same as in g , provided the dip angle δ is accurately measured. The fractional error in the determination of β is one-half that in g_0 for the region where their "inverse square" proportionality prevails. For slow stop-

¹¹ J. Patrick and W. H. Barkas, *Nuovo Cimento Suppl.* 23, 1 (1962).

ping particles, both \bar{l} and \bar{b} should be used. In typical bubble chamber operation, $L \approx 0.5$ at particle velocities near the minimum of ionization. Here the blob length contribution to the velocity estimate is almost negligible, but when $L < 0.25$, the blob length measurements become more valuable than the gap measurements. In fact, at nearly all velocities, \bar{b} constitutes useful information.

It has been said that this method requires "measurement of the position of each bubble," and it sometimes has been presumed, therefore, to be impractical. A "Video Track Analyzer"¹² was described several years ago, however, which by the mere press of a button displays or records \bar{l} and \bar{b} for each segment of track and their values averaged over a number of segments. This instrument has been of great value in emulsion work, particularly for tracks of high ionization where mere "blob counting" is inadequate. It can be simplified for bubble chamber use, and indeed Boser and Voyvodic¹³ have reported excellent results from a model designed specifically for bubble track application. The quantities \bar{l} , \bar{b} , and α have been studied in tracks presenting various aspects to the cameras.

The results here described were originally developed in connection with the analysis of particle tracks in sensitive emulsion, and consequently are designed to utilize emulsion track data efficiently. The most complete information obtainable from the granularity usually then is required, as the reaction kinematics and mass-estimates may depend on the values of β deduced. In the bubble chamber, the track structure remains similar, but additional information from the magnetic rigidity usually is available. The ionization then often merely eliminates alternatives, and thus reduces the computer time required for the analysis. "Good enough" estimates sometimes may suffice, and may be suggested by considerations of economy and common sense. One must, however, be on guard against throwing away too much information, or having unjustified confidence in the measurements. The most obvious simplification is simply to measure \bar{l} , which may be an excellent measure of g , and does not depend on track age. It would

¹² W. H. Barkas, Harry H. Heckman, James C. Hodges, and Jack G. Salvador, "Video Track Analysis" in *Korpuskularphotographie* (Institut für wissenschaftliche Photographie der Technischen Hochschule München, Munich, 1963). This instrument has been used extensively at the Lawrence Radiation Laboratory.

¹³ J. E. Boser and L. Voyvodic, 1966 *International Conference on Instrumentation for High Energy Physics* (Stanford University Press, Stanford, Calif., 1966).

be wise then to maintain $\alpha g < 1.4$ by lowering α as much as possible. Comparison should still be made with beam tracks to detect changes in chamber operating conditions from one expansion to the next. Beam tracks sometimes also vary in age among themselves.

A possible track parameter that has been proposed for measuring the velocity is the intensity of the signal obtained from the track in an electronic instrument such as the "spiral reader." This contains not only $z^2 C(P, T) F(\beta)$, but also the illumination of the track at its location in the chamber. It is affected by the dip of the track, track age, the photographic response, the phototube response, the geometry of the slit traversing the track, the angle between the slit and the track, the curvature of the track, the effect of crossing tracks, the presence of flare, the distance from the camera lens to the track segment, and several others. Many of these factors can be eliminated by normalizing to the beam track, which is flat in the chamber, of the same age, and which lies at the same distance from the camera as a vertex produced by it. Such a method nevertheless lacks the reliability of an estimate of g derived from objective counting and/or length measurement. The possible utility of such signals must be investigated for each instrument. Probably there are cases where such information may suffice for unambiguous decisions to be made between alternatives.

From other electronic signals, the blob density B may be deduced. At low blob densities, most of the information content of the track is then obtained, but where L falls below 0.5, B provides very little direct information regarding g or β . For the HPD system, Skillicorn has reported¹⁴ "Optimum use of ionization measurements would involve a study of the track density as a function of view, direction and position in the chamber." These variables to a large extent are superimposed on the more fundamental ones discussed above.

Only in special circumstances may the electronic information gained in kinematic analysis of bubble chamber vertices provide the specific types of data needed for accurate measurement of particle velocities. It is suggested that supplementary instrumentation, specifically designed to extract the track parameters \bar{l} and \bar{b} , normally be utilized for this purpose.

¹⁴ I. O. Skillicorn, "Mark II HPD Status," Brookhaven Rept. BHP-08-0-G (Feb., 1966).

UCR P107-42

UNIVERSITY OF CALIFORNIA
Riverside, California
Contract AEC AT(11-1)34 P107B

EXACT TREATMENT OF SEARCH
STATISTICS

David A. Evans
and
Walter H. Barkas

April, 1967

Abstract

Exact formulas have been found for the likelihood of any combinations of search statistics to result from successive scans of the same "area". The formulas apply for similar events which are found with arbitrary efficiencies. One obtains a best estimate of the actual number of events present and simultaneously the interval corresponding to any particular level of confidence.

EXACT TREATMENT OF SEARCH STATISTICS

David A. Evans and Walter H. Barkas

The following statistical analysis was developed to enable more information to be obtained from the results of successive scans of nuclear track emulsion or bubble chamber film. The method, however, is equally applicable to any form of search process (with replacement) which is repeated one or more times and may be described by the statistical models assumed in the present treatment.

Frequently in the field of experimental high energy physics employing track detection methods (bubble chamber, nuclear emulsion, spark chamber) the experimenter must rely on the work of scanners who search for specified types of events in the presence of large quantities of extraneous information. It is therefore to be expected that not all events of the required type will be found, i.e. the scanning process is not 100% efficient. Estimates of the efficiencies often have been made by performing a second completely independent scan. If a and b are the numbers of similar events found in the first and second scans respectively and γ is the number of events in common to the two scans then a simple argument establishes an estimate of \bar{N} the total number of events present as

$$\bar{N} = \frac{ab}{\gamma}$$

and the efficiencies of the two scans as $\epsilon_1 = \frac{a}{\bar{N}} = \frac{\gamma}{b}$, $\epsilon_2 = \frac{b}{\bar{N}} = \frac{\gamma}{a}$ respectively. However, these formulae may only be reliably applied in the case of large statistics and reasonably high efficiencies.

A closer statistical analysis of this scanning problem will be described and an attempt made to extract as much useful information as possible from the data obtained in performing two or more scans.

The situation for two scans is represented diagrammatically in fig. 1. The main area represents the number of events actually present (n), the result of successive scans (called A and B) is to enclose areas representing events seen, the intersection of these areas are events seen in common, the outside area is the missed events. All events may be divided into four exclusive classes:

- 1/ Seen by A and B, (γ)
- 2/ Seen by A not by B, (α)
- 3/ Not seen by A, seen by B, (β)
- 4/ Not seen by either A or B, ($n - (\alpha + \beta + \gamma)$)

The quantities in brackets represent the number of that type of event present. α , β , γ are experimental quantities, n is, of course, unknown. Clearly, $a = \alpha + \gamma$, $b = \beta + \gamma$ where a and b were defined previously. A further convenient quantity is $f = \alpha + \beta + \gamma$, the total number of events found.

One now postulates two quantities ϵ_A , ϵ_B which are the probabilities for A and B respectively to detect a required event. The important assumption is made that all events are equally likely to be seen. If one has reason to believe that certain event parameters such as track ionization, event geometry, etc. cause a variation in what might be termed the intrinsic probability of being seen, then events should be grouped into

bins of the parameters within which this intrinsic probability is likely to remain constant. The postulated quantities ϵ_A , ϵ_B are then the products of this intrinsic probability and the true scanning efficiencies.

With these assumptions in mind, the double scanning process may be described statistically as follows. In the first scan (A), a events are selected out of n present (n is unknown) with ϵ_A being the probability of selecting an event. The total probability is then described according to the binomial distribution as:

$$p_1(a|n, \epsilon_A) = \frac{n!}{a!(n-a)!} \epsilon_A^a (1-\epsilon_A)^{n-a}$$

The subsequent scan (B) may be divided into two sections:

- i) B's scan of events already seen by A,
- ii) B's scan of events not seen by A.

In the first case, we have the probability given as

$$p_2(\gamma|a, \epsilon_B) = \frac{a!}{\gamma!(a-\gamma)!} \epsilon_B^\gamma (1-\epsilon_B)^{a-\gamma}$$

since γ events are found out of a, with the probability per event of ϵ_B . The second case yields the probability,

$$p_3(\beta|n-a, \epsilon_B) = \frac{(n-a)!}{\beta!(n-a-\beta)!} \epsilon_B^\beta (1-\epsilon_B)^{n-a-\beta}$$

since out of (n-a) events β are found. The joint probability of the whole sequence occurring, i.e. a events by A, b events by B and γ in common is given by the product

$$p(a, b, \gamma|n, \epsilon_A, \epsilon_B) = p_1 p_2 p_3$$

Simplification of the expression yields:

$$P(a, b, \gamma) = \frac{n!}{(n-f)!} \epsilon_A^a \epsilon_B^b (1-\epsilon_A)^{n-a} (1-\epsilon_B)^{n-b} \frac{1}{\alpha! \beta! \gamma!}$$

where α, β, γ, f are as defined previously. The expression is seen to be symmetrical in a, b as it must since both scans are on an equal footing.

The above expression may be interpreted as the likelihood of a given situation of known a, b, γ with parameters $n, \epsilon_A, \epsilon_B$

$$\mathcal{L}(n, \epsilon_A, \epsilon_B | a, b, \gamma) = P(a, b, \gamma)$$

The values of these parameters which simultaneously maximize the likelihood are then the maximum likelihood estimates. It is quite easy to show that the estimates of ϵ_A and ϵ_B are $\frac{a}{n}$ and $\frac{b}{n}$ as expected, but the estimate of n cannot be obtained analytically.

In most situations n is the parameter which is desired; both its estimate and the statistical error. Accordingly, the other two parameters (the efficiencies) may be treated as "nuisance parameters" and be integrated over.⁽¹⁾ This then yields a likelihood function of the single parameter n , viz,

$$\mathcal{L}(n) = \frac{n!(n-a)!(n-b)!}{(n-f)! [(n+1)!]^2} \frac{a!b!}{a!\beta!\gamma!}$$

This expression is not very suitable for numerical evaluation since it involves the products and quotients of very large numbers (the factorials). The result may be recast in the form of the recurrence relation,

$$\mathcal{L}(n) = \frac{n(n-a)(n-b)}{(n-f)(n+1)^2} \cdot \mathcal{L}(n-1)$$

This relation is well-suited both to hand calculation and particularly to computer use. Clearly the lower limit of n is f (the total number of events found). One may arbitrarily assign $\mathcal{L}(f) = 1$ and proceed stepwise to generate as much of the likelihood function as desired. A computer subroutine using this method has been written for use when many calculations must be made (e.g. each bin of an energy spectrum). For individual problems the likelihood function may be conveniently generated with a hand calculator. The behavior of the function for the typical experimental situations is shown in fig. (2). The examples include artificial cases of small statistics to demonstrate the information still available. A confidence interval for n may be established by quoting the value $n = N$ for which

$$\sum_{n=f}^N \mathcal{L}(n) = C \sum_{n=f}^{\infty} \mathcal{L}(n),$$

where C is the confidence level desired. In practice $\sum_{n=f}^{\infty} \mathcal{L}(n)$ may be approximated by summing until further terms become a predetermined small fraction of the sum. (The nature of the convergence of the sum ensures this to be a good approximation.) The confidence level as described is, of course, single-sided.

The estimation of the individual efficiencies is best done independently. One notes that for scanner A, of the b events known to be present (found by B) only γ are found. The probability for A to detect an event is ϵ_A ; the statistical model which is appropriate is the binomial with parameter ϵ_A .

where

$$p(\gamma) = \frac{b!}{\gamma!(b-\gamma)!} \epsilon_A^\gamma (1 - \epsilon_A)^{b-\gamma}$$

It may be shown (2) that the random variable $\sin^{-1} \sqrt{\left(\frac{\gamma}{b}\right)}$ is more nearly normally distributed than γ , with mean $\sin^{-1} \sqrt{\epsilon_A}$ and variance $\frac{1}{4b}$. Hence the estimate of ϵ_A is $\frac{\gamma}{b}$ and the (two-sided) confidence interval limits are given by:

$$\sin^2 \left[\sin^{-1} \sqrt{\left(\frac{\gamma}{b}\right)} \pm \alpha \cdot \frac{1}{2\sqrt{b}} \right]$$

where α is the number of standard deviations each side of the mean for the desired confidence interval in a normal distribution (e.g. 95% conf, $\alpha = 1.96$). It is clear that the calculation for ϵ_B is identical in nature.

Extension to more than two scans

The approach leading to the expression for $\mathcal{L}(n, \epsilon_A, \epsilon_B | a, b, \gamma)$ may be extended to three or more scans of the same area. The proof is given in the Appendix and the results quoted here. Again, the recurrence relations are well suited to hand or computer calculation.

3 scans. If total number of events found is f , and each scanner finds a, b, c respectively, then:

$$\mathcal{L}_3(n, \epsilon_A, \epsilon_B, \epsilon_C | a, b, c, f) \propto \frac{n!}{(n-f)!} \epsilon_A^a \epsilon_B^b \epsilon_C^c \lambda_A^{n-a} \lambda_B^{n-b} \lambda_C^{n-c} \text{ where } \lambda = 1 - \epsilon$$

Which gives on integrating out $\epsilon_A, \epsilon_B, \epsilon_C$

$$\mathcal{L}_3(n) \propto \frac{n!}{(n-f)!} \frac{(n-a)!(n-b)!(n-c)!}{[(n+1)!]^3}$$

or
$$\mathcal{L}_3(n) = \frac{n}{n-f} \cdot \frac{(n-a)(n-b)(n-c)}{(n+1)^3} \cdot \mathcal{L}_3(n-1), \quad n \geq f$$

N scans. If total number of events found is f and the individual scans find a_i , $i = 1, 2, \dots, N$

$$\mathcal{L}_N(n, \epsilon_i | a_i, f) \propto \frac{n!}{(n-f)!} \prod_{i=1}^N \epsilon_i^{a_i} \lambda_i^{n-a_i}$$

On integrating out $\epsilon_1, \epsilon_2, \dots, \epsilon_N$

$$\mathcal{L}_N(n) \propto \frac{n!}{(n-f)!} \cdot \prod_{i=1}^N \frac{(n-a_i)!}{(n+1)!}$$

or

$$\mathcal{L}_N(n) = \frac{n}{n-f} \cdot \frac{\prod_{i=1}^N (n-a_i)}{(n+1)^N} \cdot \mathcal{L}_N(n-1)$$

References

1. D. V. Lindley, Introduction to Probability and Statistics, Cambridge University Press 1965, Vol. 2, p. 38.
2. Op. Cit. Vol. 1, p. 138.

Appendix

In order to treat the general case of N scans it is useful to introduce the following notation. The events may be divided into classes characterized by whether or not the event was seen in successive scans. Thus A will denote the class seen by A, \bar{A} the class not seen by A. Such combinations as AB, $A\bar{B}$ denote the intersections of the classes, viz. $A\bar{B}$ is the class of events seen by A and not by B. The number of events in a given class is denoted by enclosing the class symbol in square brackets. In this notation the following correspondences with the quantities defined in the main text are noted. $a = [A]$, $b = [B]$, $\alpha = [A\bar{B}]$, $\beta = [\bar{A}B]$, $\gamma = [AB]$. It is clear that relations such as

$$[A\bar{B}] + [AB] = [A]$$

hold, and in particular $[A] + [\bar{A}] = n$ the total number of events present. This notation is easily extended to cover any number of scans.

The expression for the likelihood derived in the main text for two scans may be written:

$$\mathcal{L}_2 = \frac{n!}{[AB]![\bar{A}B]![A\bar{B}]![\bar{A}\bar{B}]!} e_A^{[A]} e_B^{[B]} \lambda_A^{[A\bar{B}]} \lambda_B^{[\bar{A}B]}$$

Since $n-f = [\bar{A}\bar{B}]$ i.e. the number of events found in neither scan. The form of the denominator should be noted, viz. the product of the factorials of the numbers in each of the four classes into which the two scans divided the events. A third scan may be considered as dividing each of these classes into two, seen or not seen by C, e.g. $A\bar{B}$ is split into $A\bar{B}C$ and $A\bar{B}\bar{C}$. The

scanning of each of the four classes gives rise to an extra binomial probability factor in the likelihood, thus:

<u>Class</u>	<u>No. seen by C</u>	<u>Probability</u>
AB	[ABC]	$\frac{[AB]!}{[ABC]![ABC\bar{C}]!} \epsilon_C^{[ABC]} \lambda_C^{[ABC\bar{C}]}$
\overline{AB}	[\overline{ABC}]	$\frac{[\overline{AB}]!}{[\overline{ABC}]![\overline{ABC\bar{C}}]!} \epsilon_C^{[\overline{ABC}]} \lambda_C^{[\overline{ABC\bar{C}}]}$

and similarly for classes \overline{AB} , \overline{AB} . It is then noted that each of the four expressions contains factors like [AB]! in the numerator which cancel those present in the denominator of \mathcal{L}_2 . Further, the exponent of ϵ_C is

$$[\overline{ABC}] + [\overline{ABC}] + [ABC] + [\overline{ABC}] = [C]$$

since all possible arrangements of A, B, \overline{A} , \overline{B} occur. Similarly, the exponent of λ_C is $[\overline{C}]$. Thus one obtains

$$\mathcal{L}_3 = \frac{n!}{[ABC]! \dots [\overline{ABC}]!} \prod_{i=A, B, C} \epsilon_i^{[i]} \lambda_i^{[\overline{i}]}$$

where there are eight factors in the denominator, each corresponding to one of the eight classes into which the three scans divide the events. This should be compared with the similar expression for two scans.

Since the likelihood is a function only of n, ϵ_A , ϵ_B , and ϵ_C , all but one of the denominator factors remain constant with varying n. The exception is $[\overline{ABC}] = n-f$, the total number of events missed. Thus, rewriting [A] = a etc. one obtains

$$\mathcal{L}_3(n, \epsilon_A, \epsilon_B, \epsilon_C) \propto \frac{n!}{(n-f)!} \epsilon_A^a (1-\epsilon_A)^{n-a} \epsilon_B^b (1-\epsilon_B)^{n-b} \epsilon_C^c (1-\epsilon_C)^{n-c}$$

The situation where M scans have been done is now considered.

The extension from \mathcal{L}_2 to \mathcal{L}_3 suggests that:

$$\mathcal{L}_M = n! \prod_{i=1}^M \epsilon_i^{[i]} \lambda_i^{[\bar{i}]} \cdot \frac{1}{2^M \prod [X]!}$$

where the product $\prod [X]!$ is taken over all the 2^M classes created by the M scans.

If one now considers a further scan, this will divide each class into two. Take one class X where X denotes some combination of symbols such as \overline{ABCD}, \dots . In the new scan, $[X, M+1]$ events are seen out of $[X]$. Thus this gives a probability factor of

$$\frac{[X]!}{[X, M+1]! [\overline{X, M+1}]!} \epsilon_{M+1}^{[X, M+1]} \lambda_{M+1}^{[\overline{X, M+1}]}$$

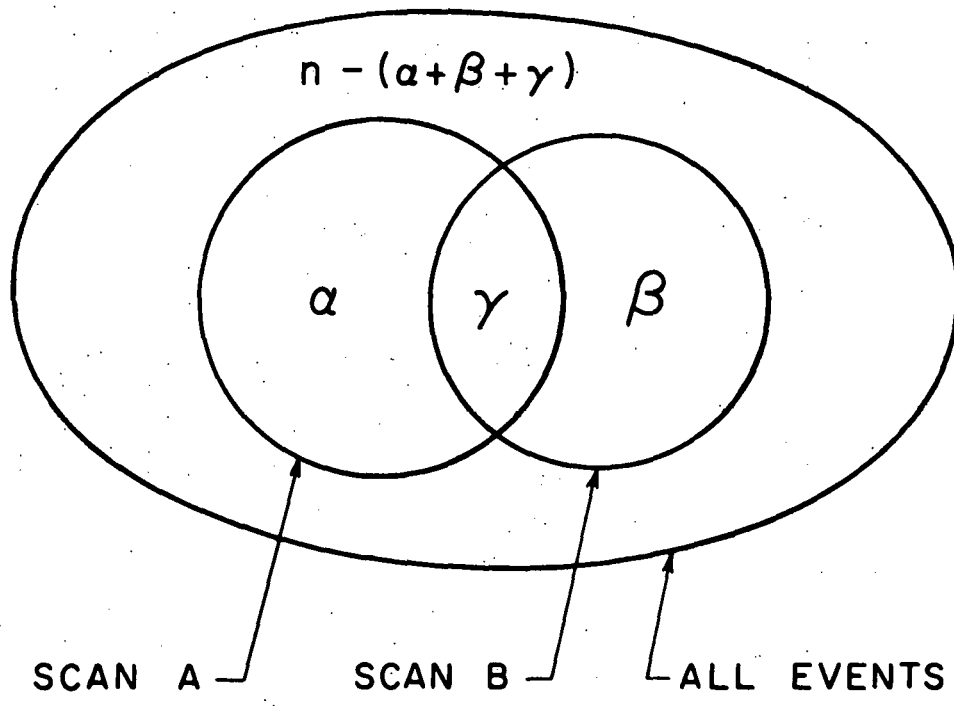
A similar expression will occur for each of the 2^M classes. When the product of all these is taken with \mathcal{L}_M the product of 2^M factors in \mathcal{L}_M cancels with the terms like $[X]!$, and is replaced by a new product over the new 2^{M+1} classes. The exponent of ϵ_{M+1} is symbolically expressed as $\sum_X [X, M+1] = [M+1]$ similarly the exponent of λ_{M+1} is $[\overline{M+1}]$. Thus,

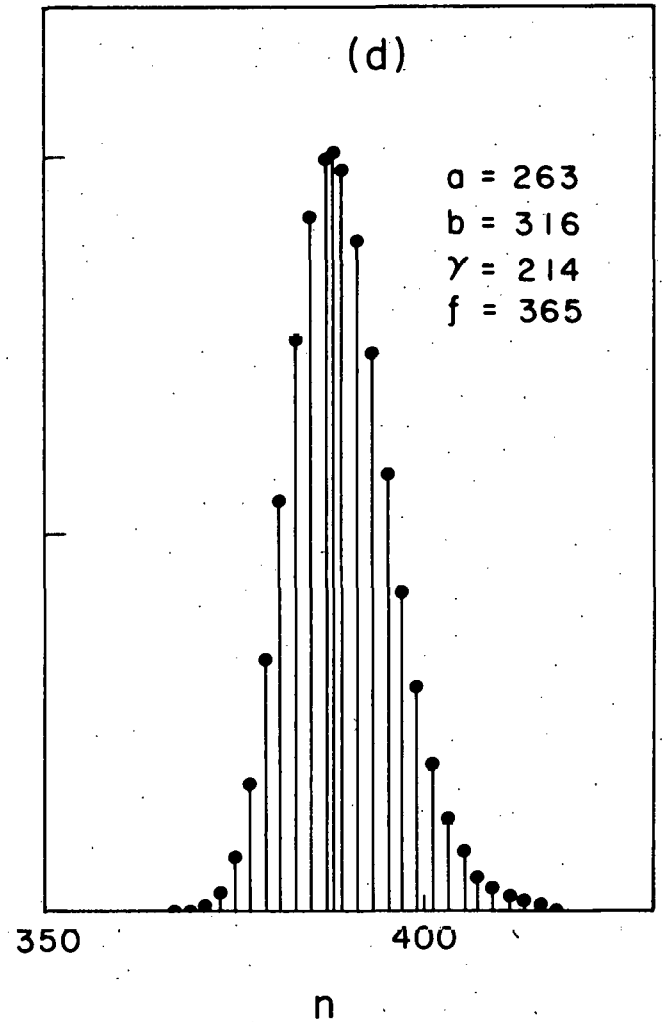
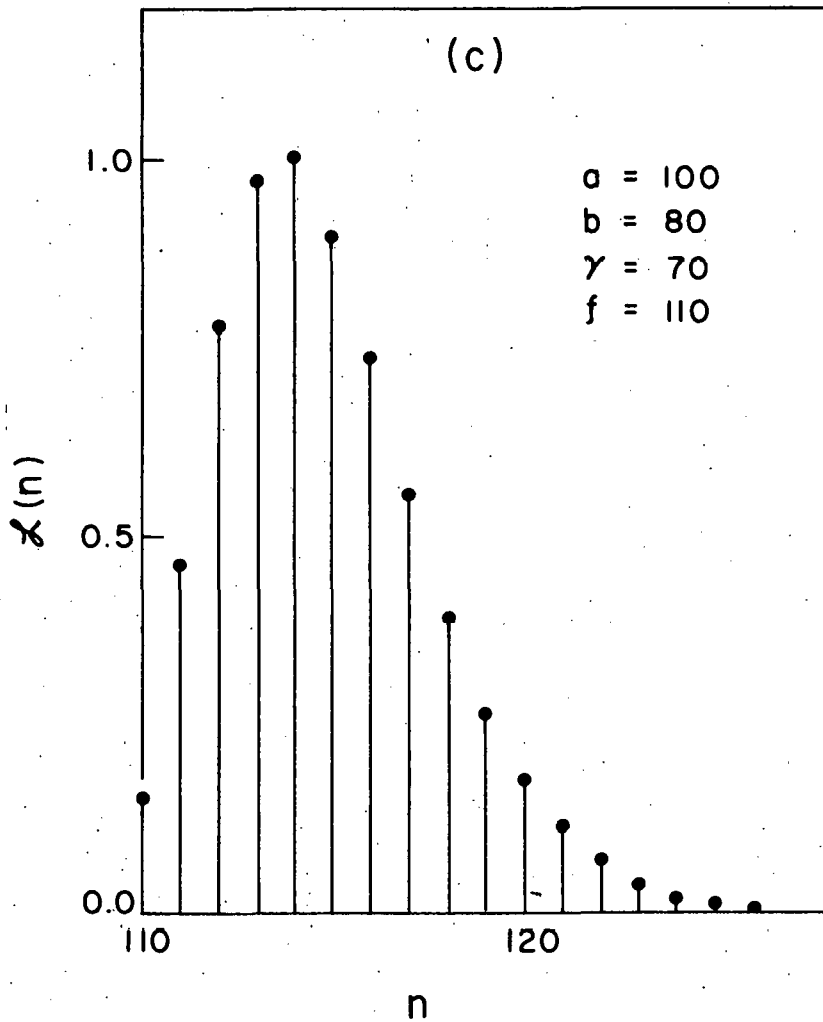
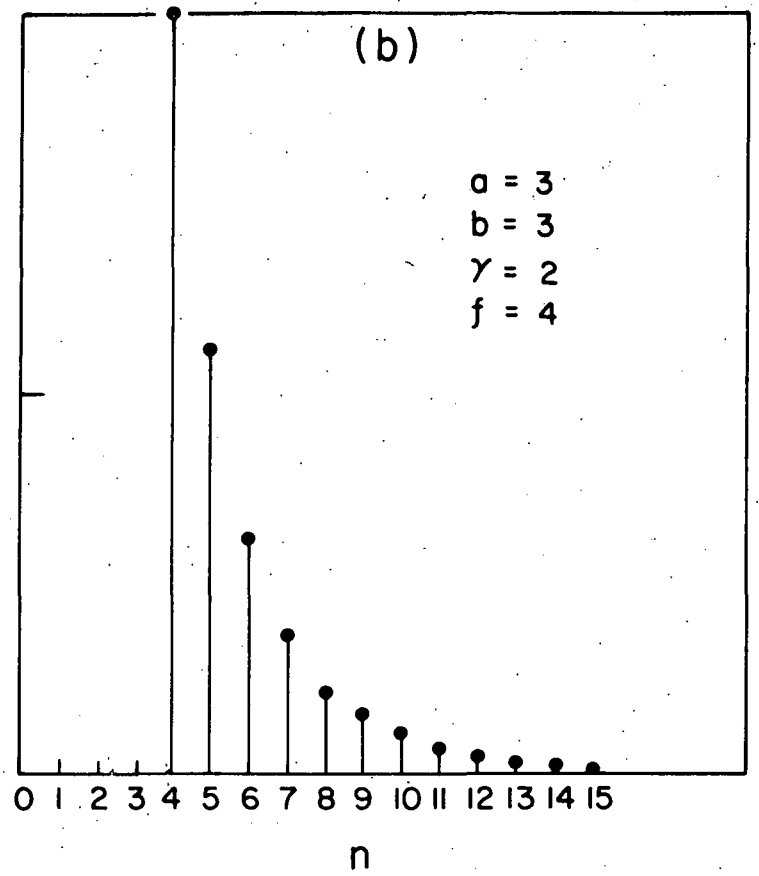
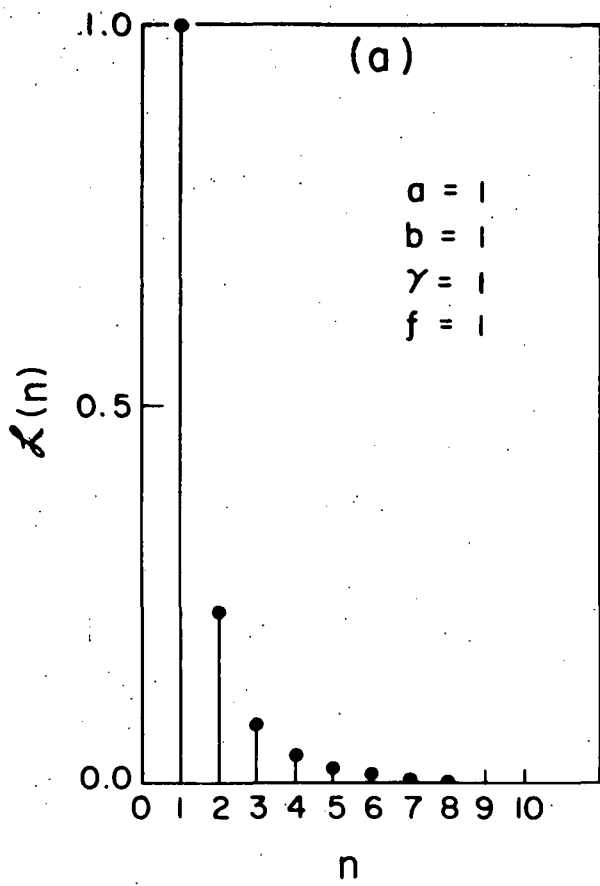
$$\mathcal{L}_{M+1} = n! \prod_{i=1}^{M+1} \epsilon_i^{[i]} \lambda_i^{[\bar{i}]} \cdot \frac{1}{2^{M+1} \prod [X']!}$$

(where X' are the 2^{M+1} new classes) i.e. the same expression as for \mathcal{L}_M with $M+1$ substituted for M . It has been shown that this general expression is true for $M=2$, therefore, by induction it is universally true.

Figure Captions

1. Diagrammatic representation of classes created by two scans. The symbols in each area are the number of events in that class.
2. Typical likelihood functions obtained using the method described. The a , b , and γ have the same meanings as in the text. The functions are normalised to $L_{\max} = 1$.





UCR P107-38

UNIVERSITY OF CALIFORNIA
Riverside, California
Contract AEC AT(11-1)34 P107B

THE PION RANGE-ENERGY CURVE IN THE REGION
USEFUL FOR MESONIC DECAY OF HYPERNUCLEI

Cliff Fok and Walter H. Barkas

February 9, 1967

The Pion Range-Energy Curve In The Region Useful For
Mesonic Decay Of Hypernuclei

Cliff Fok and Walter H. Barkas

Dept. of Physics, University of California, Riverside

In a recent study of hypernuclear binding energies¹ a disagreement was found between the values obtained from different decay modes of Λ H⁴. The effect suggests a possible error in the shape of the emulsion range-energy curve².

The present work was undertaken to test this hypothesis. A self-consistent procedure was used which exploits the fact that the prong energies in τ -meson decay are determined by the prong to prong angles. These angles were obtained by (x, y, z) coordinate measurements with automatic equipment at the decay vertex, and on each track. The ranges were measured with the same equipment; each track was broken down into essentially straight segments, the end coordinates of which were measured.

For low pion energies the absolute error in the pion energy, as determined from its range, cannot be large. This is fortunate because in this region the other two π -meson tracks are nearly collinear, and the energy cannot be determined reliably. For pions above 10 MeV the angle measurement becomes a less serious source of error, and some 127 such tracks were measured. For each track the quantity $\Delta = \frac{\text{Measured Range} - \text{Tabulated Range}}{\text{Measured Range}}$ was calculated. The tabulated ranges were deduced from Table 10.4.1 of reference 2 using a pion/proton mass ratio of 0.14878. The mean value of Δ and the standard deviation of its mean was

calculated for 10 MeV energy intervals, taking the τ meson Q value to be 75.04 MeV³. The results are as follows

Energy Interval MeV	Δ
10-20	0.0058 \pm 0.0120
20-30	-0.0039 \pm 0.0051
30-40	0.0060 \pm 0.0075
40-50	0.0048 \pm 0.0054

It seems clear that in the experiment we have not established a significant deviation of the measurements from the range-energy data in general use. While the range-energy curve surely varies smoothly with the energy, the deviations do not have a monotonic trend, nor are they anomalous compared to their standard deviations. The result is, nevertheless, somewhat marginal, because for the $\Lambda H^4 \rightarrow \pi^- + He^4$ reaction rather exceptional accuracy is required of the range-energy relation. The whole ΛH^4 effect could be explained by a local deviation near 50 MeV of about 1%.

In the decay $\Lambda H^4 \rightarrow \pi^- + He^4$, most of the Q value resides in the pion kinetic energy. The reaction has a much greater measured energy dispersion (owing to straggling of the pion range) than the competing reactions, making it intrinsically less suited for a B_Λ determination. The distribution¹ also has an unexplained skewness.

It should be realized in addition that if all ranges are measured too low by a constant factor an effect similar to that observed would ensue. Thus, if the emulsion density were higher than normal, the shrinkage factor greater than believed,

or the ranges incompletely rectified, an inconsistency such as that observed would result.

The Q values obtained from the decay modes (π^- , H^1 , H^3) and (π^- , H^2 , H^2) contain less systematic error than that from the mode (π^- , He^4). The lower pion energy-uncertainty, and the smaller anticipated errors from range-rectification and emulsion density lead to this conclusion.

¹C. Mayeur, J. Sacton, P. Vilain, G. Wilquet, D. Stanley, P. Allen, D. H. Davis, E. R. Fletcher, D. A. Garbutt, M. A. Shaukat, J. E. Allen, V. A. Bull, A. P. Conway, and P. V. March, "A Determination of the B Values of Light Hypernuclei" Bulletin #24, Institut de Physique, Universite Libre de Bruxelles.

²Walter H. Barkas, "Nuclear Research Emulsions" Academic Press, New York (1963).

³Walter H. Barkas, "Masses of the Metastable Particles" Ann. Rev. Nucl. Sci. 15, 67 (1965).

UNIVERSITY OF CALIFORNIA
Riverside, California
Contract AEC AT(11-1)34 P107B

POSSIBLE ROLES FOR EMULSION AS A DETECTOR IN
EXPERIMENTS WITH FUTURE HIGH ENERGY ACCELERATORS

Walter H. Barkas

Document prepared for presentation at the
VI International Conference on
Corpuscular Photography

July 19-23, 1966

POSSIBLE ROLES FOR EMULSION AS A DETECTOR IN
EXPERIMENTS WITH FUTURE HIGH ENERGY ACCELERATORS

Walter H. Barkas

University of California
Riverside, California

In the initial operation of the first-generation meson producing accelerators, such as the 184" cyclotron at Berkeley, emulsion as a detector had little competition. It was the only instrument that could detect mesons.

The story has been quite different with the second generation machines represented by such examples as the bevatron or the Brookhaven AGS. The areas of useful emulsion applications here have been more restricted. However, in the exploratory stages of K meson, hyperon and antiproton work, emulsion played an essential part. It still finds some areas of usefulness in this work. With first and even second generation machines, merely by putting emulsion stacks in a well prepared beam, one could sometimes do good physics. Now that technique is near its end, and arrangements more specific for the task are required. In addition very sophisticated new instruments have found their way into the physicist's bag of tricks. They can do several things that are very difficult to carry out with emulsion, despite its versatility. As it should be, the use of emulsion is confined to the jobs that it can do better than other instruments. Sometimes this means measurement of only a portion of an energy spectrum; sometimes it may depend on being able to measure small distances or simply on being

versatile. A premium is put on complete mastery of his instrument by the user so that he can capitalize on the strong points of the instrument in imaginative applications.

We are now confronted with the third generation of accelerators listed in Table I.

TABLE I

Third Generation Accelerators

	Particle	Energy	Planned date of completion
SLAC	Electron	20-40 BeV	Completed (1966)
SERPUKOV	Proton	70 BeV	1966 ?
200 BeV	Proton	200 BeV	1974
1000 BeV	Proton	1000 BeV	1981

Only a few years ago one scoffed at clashing beam devices. Now they too have to be considered third generation machines. What can we anticipate to be the areas of useful emulsion application with these new accelerators? The first answer I shall give is the official one. I quote from a document published by the Joint Committee on Atomic Energy, Congress of the United States in February 1965. It is entitled High Energy Physics Program: Report on National Policy and Background Information.

In this report on page 78 it is stated, "There are a few problems for which emulsions could be profitably employed: (1) a search for new very short-lived particles originating in nuclear stars, (2) a search for the monopole (single magnetic pole predicted

by Dirac), and (3) investigation of high energy jets, etc. Of course, it is expected that nuclear emulsions will be used routinely to study background radiations and similar technical problems around the high energy machine." This official statement seems to give emulsion only small scope. It may be a correct judgment, yet let us discuss the question at greater length.

The bubble chamber as a visual detector is nearest in principle to emulsion. The problems of the bubble chambers will be severe at high energies, but such bubble chamber men as Lynn Stevenson are now assessing the possibilities for that technique, and are coming to the conclusion that what is required are new chambers of gigantic proportions. For example, at Berkeley they are at present concerned with the optical problem of photography through six meters of liquid hydrogen. One must build chambers with linear dimensions scaled to the free paths for photon and neutron interactions in the chamber.

Can emulsion physicists, by a sufficiently brave and imaginative approach likewise extend the life of their instrument into another generation of particle physics? Is it wise? Is it worthwhile? I do not know the answers to all these questions, but I shall mention some kinds of things I think should be investigated for feasibility in connection with emulsion research programs using the new accelerators.

Suppose we consider first the strong interaction physics of the 1970's. By then most of the now-known resonant states will have been classified as to spin, parity and other quantum numbers. Much of this work will be done with bubble chambers because for

these strongly decaying states the bubble chamber is quite a suitable instrument, and in particular it is much to be preferred to emulsion. Interactions leading to more than one neutral particle in the final state will be studied, but emulsion will have nothing to contribute. Rare strong decay modes may be sought, but here again emulsion will have no part to play. High spin states will demand determination of the density matrix--again this is not a task for emulsion. It will be a difficult assignment for any instrument.

In large areas emulsion is not well adapted for strong interaction studies because it is not a simple material, because the signs and energies of the interaction products are not easily determined when the energy is high, and because the termini of tracks are so far from the interaction vertex that identification of the products is laborious, if not impossible.

At very high energies, however, mesons and other secondaries are produced in jets which defy analysis by any instrument save emulsion. An interaction with 100 secondaries can be studied in detail only with emulsion, because emulsion is the one instrument to provide high three-dimensional spatial resolution. Admittedly there remain features which are hard to measure even for emulsion, but since it has a distinct advantage over other instruments we agree with the official statement regarding the use of emulsion to study jets. We obviously should exploit this feature and develop new techniques of analysis.

We know that the meson secondaries tend to have transverse momenta of only a few hundred MeV/c. This means that in the CM system we may expect strong interaction secondaries to be largely

in the range where analysis by emulsion is feasible. Many types of secondary particles will be produced in clashing beam experiments for which the CM system is the natural one. The ability of emulsions to identify all the types of long-lived particles should be utilized in studying these processes. A few new metastable particles may be formed. In view of the predictions of SU₃, we may expect these to be of absolute strangeness 4, or higher, and to decay weakly.

Cosmic rays provide a means for studying processes at energies even beyond those of the most ambitious machine design. Here the machines enable us to calibrate the emulsion at moderate energies. If the theoretical formulas turn out to be reliable at machine energies, they can be applied with some confidence at cosmic-ray energies.

Detailed knowledge of the behavior of the grain density curve beyond the minimum is rather essential information, and errors in the scattering sagitta caused by distortion and spurious scattering must be minimized. For this a paper submitted by James Burwell to this conference is important. It would be an unhealthy turn of events, however, if with the new machines we became preoccupied with emulsion imperfections to the neglect of particle physics.

In another area emulsion may prove to have advantages. Peripheral production processes in which the nucleus does not disintegrate and to which there is little momentum transfer are easily recognized in the emulsion. These events lead to particular meson states which may be profitably studied.

Super high-energy physics with emulsion detection also can turn away from strictly particle physics to an area where emulsion has great advantages. We can study the nuclear physics of extreme

energies with beams of known character and energy. The primary and secondary interactions, the mechanism of the cascade, the theories of shock waves in nuclear matter, all may be worthy subjects of study. The scope of the work may be greatly enlarged by the introduction of external magnetic analysis and targets of pure materials. Then the physics of nucleon clusters as products of the disintegrations may be extensively analysed.

It is well known in physics research that after the quick exploration of an area is completed the real work begins. In most of high energy physics we are now in that stage. It is now time to plan the precision experiments with carefully engineered apparatus to make refined measurements of mass differences, branching ratios, magnetic moments and so forth. One lacks imagination who cannot see many possibilities for experiments in which emulsion is the best instrument for the task, and others for which it is competitive. There remain also many loose ends--unexplored areas where emulsion can be used profitably. I cite as examples studies of hyperfragment production by Σ , Ξ , and Ω hyperons.

In some areas emulsion is not competitive because although it yields results with very little systematic error, the data suffer from poor statistics. For this, one direction in which progress can be made is in the development of automatic equipment. The analyzing capacity of emulsion also is greatly enhanced when it is placed in a magnetic field of several hundred thousand gauss. New magnet techniques can be utilized to develop such fields for routine use.

Use of emulsion in conjunction with spark chambers has been

pioneered by Burhop and his collaborators. To perform the significant experiments of the future clever combinations of emulsion with other instruments will be necessary for highly specific particle detection schemes.

Let us turn now to electromagnetic and weak processes. We have theory, well developed by Pinkau and others, relating the measurable features of an electromagnetic cascade with the incident photon or electron energy. As with all theory, this needs checking and correction. Some of the finer statistical features of the cascades can best be studied empirically in any case. One approach which could be more highly developed is that of the emulsion chamber. Almost endless variations of this technique are possible.

The collision cross sections of all very energetic particles with electrons can be studied by the delta ray spectra observed. Of course, this is easier to do with a bubble chamber, but the accelerators will provide a means of calibration so that emulsion measurements with cosmic-ray particles of even higher energies will be reliable.

In addition the trident free paths for electron-pair production by fast electrons, muons and other particles will be interesting quantities to measure as functions of energy. At high energies the electromagnetic form factors of the incident particles thus will become accessible to study.

It may be possible to improve the π^0 lifetime measurements and to extend them to Σ^0 and η meson decay rates.

Of course the search for the magnetic monopole and for quarks should be continued. Indeed, the importance of the quark search

intensifies the need for more sensitive emulsions capable of detecting tracks ionizing $1/9$ the present minimum.

Most other instruments, such as the bubble chamber, find it difficult to detect and measure particles of roughly 10 MeV or less. This part of each spectrum is accessible only to emulsion for measurement. Sometimes this may be a very important region as in the τ' mode of K^+ meson decay.

Whole new families of hypernuclei containing more than one hyperon will become available for study when methods for clean separation of Ξ and Ω hyperons are developed. The general improvement in yield of such hyperons with increasing energy and the gradual development of improved technology insures that we ultimately will possess such beams. Excited states of hypernuclei also is a topic that is virtually undeveloped at present, but one which emulsion physicists would do well to develop, particularly in view of the monopoly emulsion has in this field.

The study of photonuclear reactions in the many BeV range may produce surprises. Electrodisintegration of nuclei by extremely high energy electrons may also reveal unexpected features and such studies should be carried out when feasible.

Particle states that are at present unknown because they decay electromagnetically in the lifetime interval 10^{-11} to 10^{-16} seconds may well be observed. They should be found in the vicinity of emulsion stars produced perhaps by very high energy beams of strange particles.

Detailed study of neutrino interactions in emulsion has become possible by the methods of Burhop's group at CERN. This may become

even more important as the energy is increased. A most significant experiment would be to search for the hypothetical boson, the carrier of the weak interaction. Its production might be expected in emulsion by neutrinos of sufficiently high energy. Detection of hyperons and other strange particles produced by neutrino beams also is a challenging prospect.

In view of the various problems that are open to study by means of emulsion, it seems unquestionable that the new machines will offer the opportunity for a modest but interesting program of emulsion research.